Neurobiology of Stress 18 (2022) 100451

Contents lists available at ScienceDirect

Neurobiology of Stress

journal homepage: www.elsevier.com/locate/ynstr

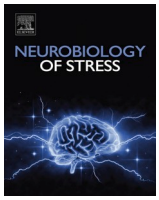

Effects of chronic social stress on oligodendrocyte proliferation-maturation and myelin status in prefrontal cortex and amygdala in adult mice

Giulia Poggi [a,**], Jamie Albiez [a], Christopher R. Pryce [a,b,*]

[a] Preclinical Laboratory for Translational Research Into Affective Disorders, Department of Psychiatry, Psychotherapy and Psychosomatics, Psychiatric Hospital, University of Zurich, Switzerland
[b] Neuroscience Center Zurich, University of Zurich and ETH Zurich, Switzerland

ARTICLE INFO

Keywords:
Chronic social stress
Medial prefrontal cortex
Amygdala
Oligodendrocyte
Myelin

ABSTRACT

Stress-related neuropsychiatric disorders present with excessive processing of aversive stimuli. Whilst underlying pathophysiology remains poorly understood, within- and between-regional changes in oligodendrocyte (OL)-myelination status in anterior cingulate cortex and amygdala (ACC-AMY network) could be important. In adult mice, a 15-day chronic social stress (CSS) protocol leads to increased aversion responsiveness, accompanied by increased resting-state functional connectivity between, and reduced oligodendrocyte- and myelin-related transcript expression within, medial prefrontal cortex and amygdala (mPFC-AMY network), the analog of the human ACC-AMY network. In the current study, young-adult male C57BL/6 mice underwent CSS or control handling (CON). To assess OL proliferation-maturation, mice received 5-ethynyl-2′-deoxyuridine via drinking water across CSS/CON and brains were collected on day 16 or 31. In mPFC, CSS decreased the density of proliferative OL precursor cells (OPCs) at days 16 and 31. CSS increased mPFC myelin basic protein (MBP) integrated density at day 31, as well as increasing myelin thickness as determined using transmission electron microscopy, at day 16. In AMY, CSS increased the densities of total $CC1^+$ OLs (day 31) and $CC1^+/ASPA^+$ OLs (days 16 and 31), whilst decreasing the density of proliferative OPCs at days 16 and 31. CSS was without effect on AMY MBP content and myelin thickness, at days 16 and 31. Therefore, CSS impacts on the OL lineage in mPFC and AMY and to an extent that, in mPFC at least, leads to increased myelination. This increased myelination could contribute to the excessive aversion learning and memory that occur in CSS mice and, indeed, human stress-related neuropsychiatric disorders.

1. Introduction

Prolonged exposure to uncontrollable aversive life events can have detrimental effects on physical and mental health (McEwen et al., 2015), including triggering and maintaining psychiatric illnesses such as major depressive disorder (MDD), generalized anxiety disorder (GAD) and post-traumatic stress disorder (PTSD) (Lupien et al., 2009; McEwen et al., 2015). These disorders (which are often comorbid) present with excessive processing of aversive stimuli and events (Friedman et al., 2011). The anterior cingulate cortex (ACC) and amygdala (AMY) contribute to the brain circuit/network responsible for aversive emotional processing (Rolls, 2019). Subregions of the ACC, namely subgenual (sgACC) and pregenual (pgACC) ACC, are both connected bidirectionally with the AMY, and these circuits contribute to aversion processing, including Pavlovian aversion learning-memory and subsequent extinction (Sehlmeyer et al., 2009). Using fMRI, changes in functional connectivity within and between ACC and AMY have been described for MDD, GAD and PTSD (Drevets, 2001; Hughes and Shin, 2011; Kim and Whalen, 2009). Whilst the cellular pathophysiology of these stress-related disorders is poorly understood, several diffusion tensor imaging (DTI) and post-mortem histological studies have, in addition to neurons and other glial systems, identified alterations in the status of oligodendrocytes (OLs) and myelination within and between ACC-AMY. These include changes in white matter tracts, myelin status, OL lineage cell density, and expression of OL-related genes and proteins (Bierer et al., 2015; Birey et al., 2015; Guilloux et al., 2012; Hamidi

* Corresponding author. PLaTRAD, Department of Psychiatry, Psychotherapy and Psychosomatics, Psychiatric Hospital, University of Zurich, August Forel-Strasse 7, CH-8008, Zürich, Switzerland.
** Corresponding author.
E-mail addresses: giulia.poggi@bli.uzh.ch (G. Poggi), christopher.pryce@bli.uzh.ch (C.R. Pryce).

https://doi.org/10.1016/j.ynstr.2022.100451
Received 22 December 2021; Received in revised form 13 April 2022; Accepted 16 April 2022
Available online 20 April 2022

et al., 2004; Harrison, 2002; Mosebach et al., 2013; Seney et al., 2018; Sibille et al., 2009; Tanti et al., 2019). The direction of reported changes is not always consistent across studies, and some also report no change in OL density and myelin content (Lutz et al., 2017; Rajkowska et al., 2015). Nevertheless, the overall evidence suggests that stress-related psychiatric disorders are associated with changes in OL lineage cell density and loss of myelin integrity, which might contribute to the connectivity changes in ACC-AMY and thereby to the pathophysiology of these severe illnesses.

In vitro cellular and *in vivo* animal studies have established the essential roles of OL lineage cells and myelination in the regulation of brain circuitry/network activity. The OL lineage constitutes heterogeneous cell types that differ with respect to order of appearance in the lineage and to function (Bergles and Richardson, 2016): In adulthood, oligodendrocyte precursor cells (OPCs) are maintained at a stable density via self-renewal. The OPCs can differentiate into mature OLs; these cells, when properly integrated into glial-neuronal networks, generate myelin (Bergles and Richardson, 2016; Dimou and Gallo, 2015; Hughes and Stockton, 2021). Myelin is a proteolipid layer that wraps neuronal axons concentrically. It is essential for metabolic support of and efficient action potential propagation along axons, thereby enabling signaling/connectivity within and between brain regions (Hirrlinger and Nave, 2014; Nave, 2010; Pajevic et al., 2014). The OL lineage and myelin both display plasticity in response to environmental inputs (Fields, 2008, 2015; Hill and Nishiyama, 2014). Several studies, primarily in rodents, have demonstrated that perturbations of the environment, including acute and chronic aversive stimulation, lead to changes in the OL lineage and/or myelin, in cortical and sub-cortical regions. Integration of these studies with human findings is facilitated by taking account of the structural-functional analogy between primate bidirectional ACC-AMY pathways and rodent medial prefrontal cortex (mPFC, prelimbic (PrL) and infralimbic (IL) cortices)-AMY pathways (Janak and Tye, 2015; Laubach et al., 2018). The AMY is a major region in the circuitry of Pavlovian aversion learning-memory, and PrL and IL are major regions in the mediation of Pavlovian aversion memory expression and extinction, respectively (Sierra-Mercado et al., 2011). Chronic stress in rodents, primarily chronic social defeat stress (CSDS), is reported to affect: [1] Structural-functional connectivity in the mPFC-AMY pathway, including reduction of fractional anisotropy (DTI) and resting state functional connectivity (rs-fMRI) between mPFC and AMY, and increased mPFC activation, detected via manganese-enhanced magnetic resonance imaging (Guadagno et al., 2018; Hemanth Kumar et al., 2014; Laine et al., 2017). [2] Number, density and proliferation-maturation dynamics of OL lineage cells in mPFC and AMY, including increased or decreased OPC density (Birey et al., 2015; Bonnefil et al., 2019; Luo et al., 2019; Sibille et al., 2009; Yang et al., 2016). [3] Myelination status in mPFC, including increased or decreased levels of myelination markers (Bonnefil et al., 2019; Laine et al., 2018; Lehmann et al., 2017). [4] Expression levels of OL and myelin-related transcripts and proteins in mPFC and AMY, including reduction of myelin basic protein (mRNA and protein), chondroitin sulfate proteoglycan 4 mRNA, and oligodendrocyte transcription factor 2 mRNA (Laine et al., 2018; Liu et al., 2018; Luo et al., 2019; Miguel-Hidalgo et al., 2018; Miyata et al., 2016). Thee effects apply primarily to mPFC, which has been studied more than AMY in this regard.

In adult male mice, 15-day chronic social stress (CSS), comprising continuous distal exposure to dominant, aggressive conspecifics punctuated by brief daily attack with minimal physical wounding, leads to a robust and reproducible generalized increase in aversion responsiveness, including increased Pavlovian aversion learning-memory, decreased aversion extinction and decreased two-way active avoidance, thereby providing a rodent model for the excessive aversion processing in MDD, GAD and PTSD (Adamcyzk et al., 2021; Azzinnari et al., 2014; Bergamini et al., 2018; Cathomas et al., 2019; Fuertig et al., 2016; Just et al., 2018). In these studies, in the case of behavioural, physiological and neurobiological measures, the variance within the CSS group is consistently similar to that in the control group. These CSS effects are obtained without dividing mice into sub-groups of "susceptible" (reported to be 70–80% of mice) versus "resilient" (20–30% of mice) mice based on their subsequent passive avoidance of the aggressor mouse strain, the method used in the common CSDS protocol (Golden et al., 2011). It was recently reported (Milic et al., 2021) that the behaviour of mice in tests of approach to novelty and avoidance of harm *prior* to CSDS predicts their "susceptibility" or "resilience". Accordingly, differences in the behaviour, physiology, or neurobiology between "susceptible" and "resilient" mice will depend on traits present before and states emerging after CSDS. Our approach of CSS without screening and comparison of all CSS mice with all control mice to study the "average effect" of CSS, is informed by the assumption that the mice in both groups will have different behavioural traits at the onset of the study. That is, we use an *inclusive* experimental design, as used extensively with other stressors e.g. chronic unpredictable mild stress (Tye et al., 2013; Willner, 1997). It is also important that the duration of CSS is 15 days compared with 10 days in CSDS, daily attacks are timed so that the maximum possible duration of daily attack is 1 min with CSS versus 5–10 min in CSDS, and physical wounding is minimized by trimming the teeth of aggressor mice in CSS whereas this is not the case with CSDS (Azzinnari et al., 2014; Pryce and Fuchs, 2017).

Of particular relevance to the present study, CSS leads to increased mPFC-AMY resting-state functional connectivity (Grandjean et al., 2016) and down-regulated expression of a number of OL lineage-related genes in mPFC and AMY (Cathomas et al., 2019). Based on this evidence, in the current study we deployed immunofluorescence and electron microscopy to investigate effects of CSS on mPFC and AMY status with respect to: [1] OL lineage proliferation-maturation dynamics, and [2] myelin content and ultrastructure. To investigate the progression and persistence of any CSS effects on mPFC and AMY OL lineage cells and on myelination, the post-CSS time points of 1 day and 15 days were analyzed and compared. Given the high reproducibility of CSS effects on aversion-directed behavior (see above) and the evidence that behavioral tests themselves (e.g. motor, social, sensory and learning tasks) impact on OL cell lineage and myelination status (Gibson et al., 2014; Huang et al., 2017; Hughes et al., 2018; Kato and Wake, 2021; Liu et al., 2012; McKenzie et al., 2014; Sampaio-Baptista et al., 2013; Steadman et al., 2020; Xiao et al., 2016), this study was conducted in the absence of the potential confound of behavioural testing.

2. Materials and Methods

2.1. Animals and maintenance

Two experiments were conducted with young-adult male C57BL/6J mice: In an experiment that aimed to investigate chronic social stress (CSS) effects on OL lineage fate mapping and myelin content (Expt 1), sample sizes were control (CON) n = 12 and CSS n = 14. In an experiment that aimed to investigate CSS effects on myelin ultrastructure (Expt 2), sample sizes were CON n = 6 and CSS n = 6. Mice were bred in-house and after weaning were maintained in littermate pairs in individually ventilated type 2L cages at 20–22 °C and 50–60% humidity under a reversed 12:12-h light-dark cycle (white lights off 07:00–19:00 h). Experimental procedures were conducted during the dark phase, at 10:00 to 16:00 h. Food (Complete pellet Provimi, Kliba Ltd, Kaiseraugst, Switzerland) and water were available *ad libitum*, when not stated otherwise. Resident mice for the CSS protocol were ex-breeder males of the CD-1 strain (Janvier, Saint-Berthevin, France) aged 8 months and caged singly. The study was conducted under a permit for animal experimentation (ZH093/2019) issued by the Veterinary Office of Canton Zürich.

2.2. Experimental designs

In Expt 1 (Fig. 1A), 10-week-old C57BL/6J mice were assessed for

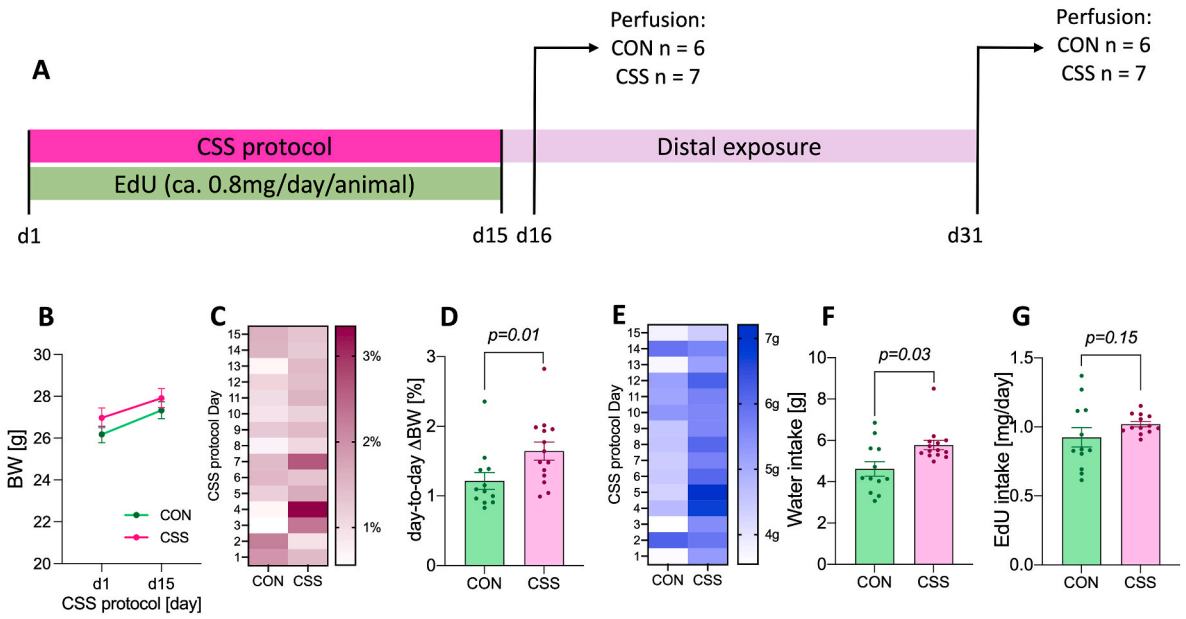

Fig. 1. Chronic social stress (CSS) compared with control (CON) mice had increased day-to-day body weight delta**, greater daily water intake and comparable daily EdU intake.** (A) Experimental design for CSS effects on oligodendrocyte lineage fate mapping. (B) Comparable increase in body weight in CSS and CON mice at day1 vs. day15 of CSS/CON protocol (2-way ANOVA repeated measures, time: $F(1,24) = 36.14$, $p < 0.0001$; group: $p \geq 0.26$). (C, D) Increase of day-to-day body weight delta ([(BW day n - BW day n-1)/BW day n-1] x 100) in CSS vs. CON mice (Mann-Whitney $U = 37$, $p = 0.01$). (E) Increased daily water intake in CSS vs. CON mice (Mann-Whitney $U = 42$, $p = 0.03$). (F) EdU concentration in drinking water was adjusted to daily water intake to ensure comparable EdU administration in CSS and CON (Mann-Whitney $U = 51$, $p = 0.15$). Data are presented as individual values and/or mean ± SEM.

locomotion, body weight and daily water intake, and these parameters were used for counterbalanced allocation to CON and CSS groups. After the 15-day CSS/CON protocol, one-half of the mice of each group was transcardially perfused on day 16, and the other half was transcardially perfused on day 31. Brains were collected for the study of OL lineage and myelin content in mPFC and AMY. In Expt 2 (Fig. S1A), 10-week-old C57BL/6J mice were assessed for locomotion and body weight, and these parameters were used for allocation to CON and CSS groups. After the 15-day CSS/CON protocol, on day 16 all mice were transcardially perfused and brains were collected for the study of myelin ultrastructure in mPFC and AMY.

2.3. Chronic social stress protocol

Chronic social stress (CSS) was conducted as described in detail previously (Azzinnari et al., 2014). Briefly, the home cages of aggressive CD-1 mice were divided by a transparent, perforated divider. For 15 consecutive days, a CSS mouse was located in the same compartment as an unfamiliar CD-1 resident mouse for either a cumulative total of 60 s physical attack or 10 min total exposure time, whichever occurred sooner. Thereafter the CSS mouse remained in the attack compartment, whilst the CD-1 mouse was transferred to the opposite compartment. The animals remained in distal exposure for the following 24h. Importantly, to prevent bite wounds during the attacks, the lower incisors of CD-1 mice were trimmed every third day. Attack time of 60 s maximum and teeth trimming eliminate the open bite wounds reported to occur in the conventional chronic social defeat protocol (Golden et al., 2011), and also minimize the occurrence of surface wounds (Azzinnari et al., 2014; Fuertig et al., 2016). Control (CON) mice remained in littermate pairs and were handled and weighed on each of the 15 days. Body weights of CSS and CON mice were recorded daily, and percentage absolute day-to-day body weight delta (ΔBW) was calculated as [(BW day n - BW day n-1)/BW day n-1] x 100. Day-to-day absolute ΔBW is consistently higher in CSS versus CON mice and provides a within-experiment physical biomarker that mice have responded to CSS (Azzinnari et al., 2014; Fuertig et al., 2016; Grandjean et al., 2016). In Expt 1, for the sub-group of mice maintained until day 31, CSS mice remained in distal exposure to the same CD-1 mice from day 16 to day 31 without any further attacks; compartment allocation within the same cage was swapped daily to maintain the stressor of sensory exposure to CD-1 mouse bedding.

2.4. EdU administration

For Expt 1, throughout the 15-day CSS/CON protocol, all mice were administered 5-ethynyl-2′-deoxyuridine (EdU; Cat. No. E10187, ThermoFisher Scientific) via the drinking water. Water intake was monitored daily for 5 days prior to the onset of the CSS/CON protocol, and EdU concentration in the drinking water was adjusted to ensure that each mouse would consume a minimum of 0.6 mg EdU per day, an amount demonstrated to efficiently label proliferative cells without any sign of toxicity (Young et al., 2013). EdU was prepared freshly every 2 days by dissolving in water at 35 °C overnight. During the CSS/CON period, water consumption was measured daily and EdU concentration adjusted as necessary (see Results). In CON mice the total water/EdU consumption per pair was used to calculate per mouse consumption by taking the respective body weights of the two mice into account and assuming that the heavier mouse would consume proportionately more. All cells that incorporated EdU are referred to collectively as the total number of proliferative cells. All OL lineage cells that incorporated EdU were assumed to be OPCs that underwent self-renewal during the period of EdU administration, and type 1 OLs or type 2 OLs derived from such proliferative OPCs (see below for nomenclature details); the collective term proliferative OL lineage cells is used to describe EdU^+ OPCs, type 1 OLs and type 2 OLs.

2.5. OL lineage and myelination markers

2.5.1. Immunofluorescence and confocal acquisition

In Expt 1, on day 16 or day 31 (Fig. 1A), mice (CON n = 6, 6; CSS n = 7, 7) were perfused transcardially with 15 mL of 1x PBS (pH 7.4) at RT followed by 50 mL of ice-cold 4% paraformaldehyde (PFA) in 0.1M

sodium phosphate buffer (pH 7.4). Perfusion rate was maintained at 20 mL/min. The brains were then removed from the skull, post-fixed for 2 h in 4% PFA at 4 °C, subsequently rinsed twice in 1x PBS and dehydrated in 30% (w/v) sucrose in 1x PBS for 48 h at 4 °C. The brains were then embedded in cryoprotecting medium (Tissue-Tek, O.C.T., Cat. No. 4583, Sakura Finetek Europe) and stored at −80 °C until further processing. Sections obtained from brains perfused on experimental day 16 or day 31 were processed in parallel.

Coronal cryo-sections (40 μm) including mPFC subregions (bregma: +2.0 mm and +1.8 mm; 1 section at each level per mouse) or basolateral amygdala (BLA, bregma: −1.4 mm and −1.8 mm) were transferred to 1x PBS and washed for 1 h (3 × 20 min) to remove any residual cryoprotective medium. EdU labelling was conducted using the Click-iT™ EdU Cell Proliferation Kit for Imaging (C10337 or C10339, ThermoFisher Scientific) according to the manufacturer's instructions, with the exception that for aspartoacylase (ASPA) staining (see below), the additive buffer was used undiluted prior to antibody staining. Sections were then blocked with 10% donkey serum in 0.5% (v/v) Trion X-100 in PBS for 1 h at RT. For simultaneous staining of the OPC marker, neuron-glial antigen 2 (NG2), and the OL marker, anti-adenomatous polyposis coli clone CC1 (CC1), respectively, the sections were incubated with rabbit polyclonal anti-NG2 (1:250; AB5320, Merck-Millipore) and mouse monoclonal anti-CC1 (1:50; OP80, Merck-Millipore), in 3% donkey serum in 0.5% (v/v) Triton X-100 for 18 h at 4 °C. On the following day, sections were incubated with fluorophore-conjugated secondary antibodies (1:500; Alexa Fluor Secondary Antibodies, Thermofisher) in 3% donkey serum in 0.5% (v/v) Trion X-100 for 2 h at RT. Sections were mounted on SuperFrost slides (10149870, ThermoFisher) and cell nuclei were stained directly by addition of DAPI Fluoroshield Mounting Medium (F6057, Merck). Cells expressed NG2 and CC1 mutually exclusively. For separate staining of the OL marker ASPA, sections were incubated in citrate buffer (pH 6.0) and heated at 96 °C for 15 min; the sections were then allowed to cool to RT during 20 min, washed 3 times in 1x PBS and then stained with rabbit polyclonal anti-ASPA/Nur7 (1:500; ABN1698, Merck-Millipore) using the above protocol. Oligodendrocyte cells that are $CC1^+$ are morphologically heterogeneous, e.g. (Fard et al., 2017). In the current study, $CC1^+$ cells were heterogenous with respect to soma size, CC1 signal intensity and colocalization of ASPA staining, and 3 different "types" were differentiated (Fig. S2A): Type 1 OL cells had relatively large soma diameter (>13 μm), high signal intensity, and no ASPA signal. With respect to morphology, these OLs resemble newly matured OLs as described in (Hughes et al., 2018; Xiao et al., 2016). Compared with type 2 OLs they were rare, and they could correspond to the 2–8% of mature $CC1^+$ OLs not detected by ASPA staining according to (Madhavarao et al., 2004). Type 2 OL cells had relatively small soma diameter (typically 8–10 μm), medium-high CC1 signal intensity, and a colocalized ASPA signal, as described in (Madhavarao et al., 2004). Both type 1 OLs and type 2 OLs were studied, and representative images are given in Fig. S2A. A third type of $CC1^+$ OL was also identified, with a highly ramified morphology, low $CC1^+$ signal intensity and negative staining for ASPA; these cells resembled those described as pre-myelinating OLs (Fard et al., 2017), and they were not quantified in the present study.

To be able to identify OL lineage cells that were EdU^+ but NG2, CC1 and ASPA negative, pilot studies were conducted for Olig2: It is often claimed that Olig2 is a pan-OL marker (eg.(Bonnefil et al., 2019; Teissier et al., 2020), although see (Nishiyama et al., 2009)). In a pilot immunostaining, a clear $Olig2^+$ signal colocalized with 95% of $NG2^+$ cells, but with only 10–15% of $CC1^+$ OLs (Figs. S3A–D). A similarly low colocalization of Olig2 with mature OLs was observed in adult mice of a *Cnp-eGFP* transgenic mouse line expressing membrane bound eGFP in CNP-expressing, and therefore mature, OLs (Fig. S3E). In the absence of availability of an alternative pan-OL marker, it was not possible to investigate directly whether the EdU^+ cells that did not express NG2, CC1 or ASPA were another maturational stage of OL lineage cells. We therefore addressed this issue indirectly by running immunostaining with the microglia markers ionized calcium-binding adapter molecule 1 (Iba1) and cluster of differentiation 68 (CD68). For microglia staining, sections were incubated with rabbit anti-Iba1 (1:500; 019–19741, Wako) and rat monoclonal anti-CD68 (1:1000, MCA1957GA, Serotec), in 3% donkey serum in 0.5% (v/v) Triton X-100 for 18 h at 4 °C. On the following day, sections were incubated with fluorophore-conjugated secondary antibodies (1:500; Alexa Fluor Secondary Antibodies, Thermofisher) in 3% donkey serum in 0.5% (v/v) Trion X-100 for 2 h at RT. Sections were mounted on SuperFrost slides (10149870, ThermoFisher) and cell nuclei were stained directly by addition of DAPI Fluoroshield Mounting Medium (F6057, Merck). Any astrocyte contribution to the pool of proliferative cells could be excluded on the basis of the findings of a previous CSS study conducted with BrdU: the following primary antibodies were used: goat anti-GFAP 1:500, ab53554, Abcam; rat anti-BrdU 1:250, ab6326, Abcam. BrdU detection required antigen retrieval, using the protocol described above for ASPA staining.

Images were acquired at a confocal laser scanning microscope Leica Sp8, with an HC PL APO CS2 20x NA 0.75 multi-immersion objective in photon counting mode for EdU, NG2 and CC1 staining, and in standard mode for EdU, IBA1 and CD68 staining. For EdU and ASPA staining, images were acquired at a confocal laser scanning microscope Leica Stellaris 5, with an HC PL APO CS2 20x NA 0.75 air objective in standard mode. The pinhole was set to 1AU, pixel size to 0.3342 × 0.3342 μm^2 and z-stack interval to 1 μm.

To assess whether CSS affected apoptosis, cleaved caspase 3 immunostaining was conducted. Sections were transferred to 1x PBS and washed for 1 h (3 × 20 min) to remove any residual cryoprotective medium. The sections were mounted on SuperFrost slides (10149870, ThermoFisher) and incubated in citrate buffer (pH 6.0) and heated up to and left at 97 °C for 10 min; the sections were then allowed to cool to RT during 30 min, washed 3 times in 1x PBS, blocked in 3% donkey serum in 0.2% (v/v) Trion X-100 in PBS for 1 h at RT, and then stained with rabbit anti-cleaved caspase 3 (1:200, #9661, Cell Signalling Technology) and counterstained with mouse anti-NeuN (1:1000, MAB377, Merck) in 2% donkey serum in 0.2% (v/v) Trion X-100 in PBS for 18 h at 4 °C. On the following day, sections were incubated with fluorophore-conjugated secondary antibodies (1:500; Alexa Fluor Secondary Antibodies, Thermofisher) in 2% donkey serum in 0.2% (v/v) Trion X-100 for 2 h at RT. Cell nuclei were stained directly by addition of DAPI Fluoroshield Mounting Medium (F6057, Merck). Images were acquired at a confocal laser scanning microscope Leica Sp8, with an HC PL APO CS2 20x NA 0.75 multi-immersion objective in standard mode. The pinhole was set to 1AU, pixel size to 0.3342 × 0.3342 μm^2 and z-stack interval to 2 μm.

For myelin content analysis using the markers myelin basic protein (MBP) and neurofilament-200 (NF200), sections were incubated in 0.5% (v/v) Triton X-100 in PBS for 90 min at RT, blocked in 5% (w/v) donkey and 5% (w/v) goat serum in 0.5% (v/v) Triton X-100 in PBS for 1 h at RT and incubated with rat anti-MBP (1:200; MCA409S, Serotec) and mouse anti-NF200 (1:200; N0142, Sigma) in 1.5% (w/v) donkey and 1.5% (w/v) goat serum for 18 h at 4 °C. On the following day, sections were incubated with fluorophore-conjugated secondary antibodies (1:500; Alexa Fluor Secondary Antibodies, Thermofisher) in 1.5% donkey and 1.5% goat serum in 0.5% (v/v) Triton X-100 for 2 h at RT. Sections were mounted on SuperFrost slides with Fluoroshield Mounting Medium. Images were acquired at a Leica Sp8, with an HXC PL APO 37 °C CS2 63x NA1.3 glycerol objective in photon counting mode; pinhole was set to 1 AU, pixel size to 0.1002 × 0.1002 μm^2 and z-stack interval to 0.3 μm.

Image acquisition was conducted within 48 h of completion of the corresponding staining protocol, with the order of image acquisition randomized across subjects to exclude occurrence of any technical bias. Fig. S4 illustrates the OL lineage cell types and myelin markers.

2.5.2. Fluorescence image analysis and quantification

Image processing and quantification in Expt 1 were performed with FIJI (Schindelin et al., 2012). For OL lineage fate mapping analysis in

mPFC (PrL and IL combined and separately) and BLA, both cell density and marker co-localization were quantified in a semi-automated manner using a custom-written macro and a FIJI co-localization plugin. For myelin content analysis in the same (sub-)regions, the mean grey value of the total field of view was calculated for each optical plane of each acquired z-stack and the optical plane with the maximum mean grey value was identified. This optical plane and the 10 optical planes above and below it were included in the analysis, so that 6 μm of the total section thickness was used for quantification. Semi-automated segmentation of MBP^+ fibers was performed via a custom-written macro and the integrated density of the MBP^+ signal was used to quantify MBP content. In order to estimate the level of apoptosis, the number of cells expressing cleaved caspase 3 per section was counted manually.

2.6. Myelin ultrastructure

2.6.1. Transmission electron microscopy

In Expt 2, on day 16, mice (CON n = 6; CSS n = 6) were perfused transcardially with 5 mL of 0.1M cacodylate buffer/0.1M sucrose, pH 7.4 at 37 °C, followed by 30 mL of 2.5% glutaraldehyde (GA, 16200, Electron Microscopy Science)/2% formaldehyde (FA, 15719, Electron Microscopy Science) in 0.1M cacodylate buffer/0.1M sucrose, pH 7.4 at RT. Coronal sections at 800 μm were prepared at the vibratome and stored in fixative at 4 °C until further processing. Micropunches of mPFC and amygdala (AMY, including BLA) tissue were obtained out of the coronal sections, incubated in 1% osmium tetroxide (OsO_4) in 0.1M cacodylate buffer followed by 1% uranyl acetate in ddH_2O, dehydrated in alcohol and ether, and embedded in Epon. After trimming the Epon block, semi-thin sections were collected and stained with methylene blue to confirm the brain region. Epon blocks were then trimmed further to prepare the specimen for ultra-thin sectioning. Sections of 60 nm were prepared with a diamond knife at the ultramicrotome (Leica Ultracut UCT OPH-045). Three of these sections were collected with a copper perfect loop and loaded onto a carbon-labelled copper grid. Three copper grids (nine sections) per region were collected per mouse. For the mPFC, a minimum of 80 micrographs were acquired at a TEM FEI CM 100 (acceleration voltage 40–100 kV, aligned for 80 kV; digital Gatan Orius 1000 as detector system). For the AMY, a minimum of 70 micrographs were acquired at a TEM FEI Tecnai G2 Spirit (acceleration voltage 40–120 kV, aligned for 120 kV; digital camera Gatan Orius 1000 as detector system). Myelin thickness (in μm and g-ratio) and myelinated axon density were quantified manually using FIJI software. Given that the non-compacted myelin compartment has been reported to exhibit changes in stress-related psychiatric disorders (Uranova et al., 2001, 2011, 2007), the myelin g-ratio was calculated excluding the non-compacted myelin compartment and the periaxonal space (Poggi et al., 2016). All the axons contained in the acquired micrographs – total ≥70 axons/region/mouse - were quantified, except for any myelinated axons that presented obvious fixation artefacts which were excluded from the analysis.

2.7. Statistics

The experimenters were blinded to the identity of the sections for all neuroanatomical image capturing and analysis. Statistical analysis was performed using GraphPad Prism. Data normality was assessed using the Shapiro-Wilk test and any outliers identified using Grubbs' test were excluded. With normally distributed data: For unpaired two-sample CSS versus CON comparisons, Student's *t*-test was used, or Welch's *t*-test in the case of unequal group variances. For analysis of group (CON, CSS) and time (day 16, day 31) effects, two-way repeated measures ANOVA was used, followed as appropriate by Tukey's or Sidak's *post hoc* test. With non-normally distributed data, unpaired two-sample group comparisons were conducted using the Mann-Whitney *U* test. Data are presented as mean ± S.E.M. and, wherever practicable, individual data points are also given in the graphs. Statistical significance was set at $p \leq 0.05$.

3. Results

3.1. CSS causes consistent changes in physical status

In Expt 1, as is typical for the CSS procedure, mice received about 45 s of daily attack and displayed submissive behavior including vocalization, across the 15-day protocol. Importantly, no deep bite wounds occurred, and a 15-day total of 2.08 ± 0.38 (mean ± SEM) small surface wounds were recorded per mouse. Body weight (BW) increased from day 1 to day 15 and comparably so in both groups (Fig. 1B, time: $F(1,24) = 36.14$, $p < 0.0001$). As expected, CSS mice presented with a higher average absolute day-to-day BW delta (ΔBW) than CON mice (Fig. 1C and D, Mann-Whitney $U = 37$, $p = 0.01$). CSS mice also had higher average daily water intake than CON mice (Fig. 1E and F, Mann-Whitney $U = 42$, $p = 0.03$). Based on this latter effect, EdU concentration in the drinking water was adjusted, such that the average daily EdU intake was similar in the two groups (Fig. 1G, Mann-Whitney $U = 51$, $p = 0.15$). In Expt 2 (Fig. S1A), BW was again higher at day 15 than day 1 of the CSS/CON protocol (Fig. S1B, time: $F(1,10) = 26.59$, $p = 0.0004$), and in this cohort the increase was greater in CSS than CON mice (group x time interaction: $F(1,10) = 12.70$, $p = 0.005$). Again, CSS mice exhibited higher average absolute day-to-day ΔBW than CON mice (Figs. S1C–D, unpaired *t*-test $t = 3.962$, $df = 10$, $p = 0.003$). The CSS-related physical and behavioral effects and the minimal surface wounding observed in both experiments were consistent with the expected outcomes for the CSS protocol (Azzinnari et al., 2014; Bergamini et al., 2018). Furthermore, in Expt 1 there was no confounding effect of CSS on EdU intake.

3.2. Chronic social stress leads to area- and stress state-specific changes in oligodendrocyte lineage density, proliferation, and maturation

Our first aim was to determine the effects of CSS on the total density of the OL lineage, directly after the 15-day protocol (day 16) and after a post-CSS period of 15 days (day 31); accordingly, we quantified the densities of $NG2^+$-OPCs, $CC1^+$ type 1 OLs and $ASPA^+$ type 2 OLs (see Material and Methods section; Fig. S2). Second, we aimed to determine the effects of CSS on OL lineage proliferation-maturation dynamics, achieved by labelling proliferative cells with EdU administered during the CSS/CON protocol specifically, and then quantifying the density of EdU^+ OL lineage cells. These quantifications were performed in mPFC (PrL and IL, combined and separately) and BLA.

3.2.1. CSS leads to decreased OPC proliferation in medial prefrontal cortex

In mPFC (Fig. 2) there was no effect of CSS or time on the total density of OPCs (Fig. 2A). For type 1 OLs, although there was a significant group x time interaction effect ($F(1,22) = 6.053$, $p = 0.02$), there was not a significant CSS effect at either time point (Tukey's multiple comparison test: d31 CSS > CON: $p = 0.09$). There was also no effect of CSS or time on type 2 OLs (Fig. 2A). CSS led to a reduction in the total number of proliferative cells in the mPFC (Fig. S5A, group: $F(1,22) = 7.086$, $p = 0.01$). OL lineage cell type-specific analysis revealed that the CSS effect on proliferation was specific to OPCs (Fig. 2B, group: $F(1,22) = 4.396$, $p = 0.05$). This did not correlate with EdU intake (Fig. S6) and co-occurred with a reduction in proliferative OPCs in both groups from day 16 to day 31 (Fig. 2B, time: $F(1,22) = 33.56$, $p < 0.0001$). Consistent with a previous report of OL lineage turnover (Young et al., 2013), about 35% of total OPCs (Fig. 2A, day 16) had proliferated ($EdU^+/NG2^+/CC1^-$) within 16 days after the onset of EdU administration (Fig. 2B, day 16), and the density of these cells was reduced by day 31 (Fig. 2B, time: $F(1,22) = 33.56$, $p < 0.0001$). There was no effect of CSS or time on the density of EdU^+ type 1 OLs (Fig. 2B). For EdU^+ type 2 OLs (Fig. 2C, $EdU^+/ASPA^+$), there was no effect of CSS and the density increased in both groups from day 16 to day 31 (Fig. 2C, time: $F(1,22) = 33.42$ $p < 0.0001$). Interestingly, in both groups at day 16, most of the

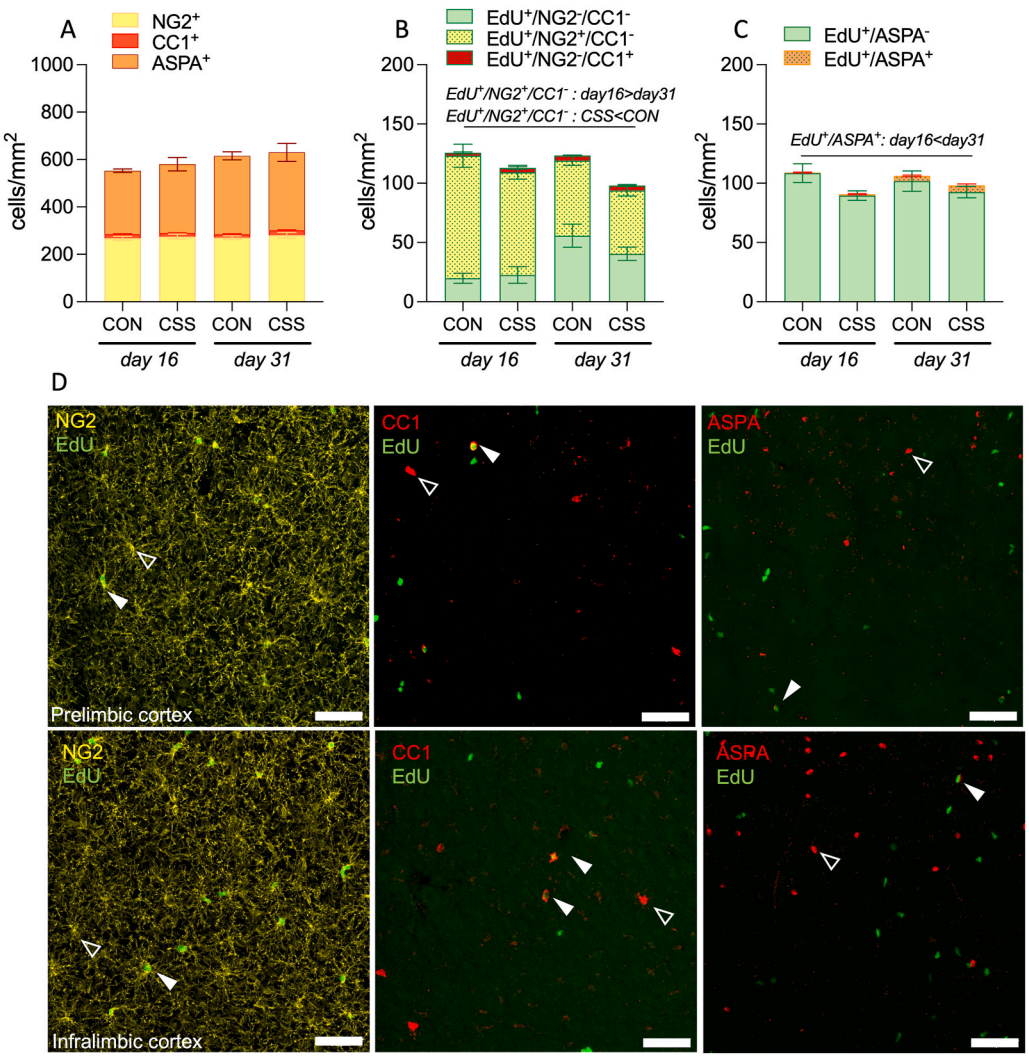

Fig. 2. Chronic social stress (CSS) leads to a reduction in OPC proliferation in medial prefrontal cortex. (A) Total densities of OL lineage cell types were comparable between groups and time points (2-way ANOVA, $NG2^+$ group: $p = 0.39$; time: $p = 0.69$; group x time interaction: $p = 0.88$. $CC1^+$ group: $p = 0.28$; time: $p = 0.41$; group x time interaction: $F(1,22) = 6.053$, $p = 0.02$. $ASPA^+$ group: $p = 0.71$; time: $p = 0.08$; group x time interaction: $p = 0.65$). (B) Density of $EdU^+/NG2^+/CC1^-$ cells was lower in CSS than CON mice and decreased from day 16–31 (2-way ANOVA, group: $F(1,22) = 4.396$, $p = 0.05$; time: $F(1,22) = 33.56$, $p < 0.0001$; group x time interaction: $p = 0.60$). Density of $EdU^+/NG2^-/CC1^+$ cells was comparable between groups and time points (group: $p = 0.53$; time: $p = 0.12$; group x time interaction: $p = 0.49$). (C) Density of $EdU^+/ASPA^+$ cells increased from day 16–31, without an effect of CSS (time: $F(1,22) = 33.42$, $p < 0.0001$; group: $p \geq 0.18$). Data are presented as mean ± SEM cells/mm^2, with values for each mouse being the mean of 2 sections x 2 subregions x 2 hemispheres. (D) Representative micrographs of the OL lineage markers in mPFC (open arrows denote OL marker, closed arrows denote OL marker and EdU). Scale bar = 50 μm. Brightness and contrast have been adjusted for display purposes.

EdU^+ OLs belonged to type 1 OLs, and the density of EdU^+ type 1 OLs was higher than the density of EdU^+ type 2 OLs (Fig. S7A, cell type: $F(1, 11) = 6.852$, $p = 0.02$). There was no difference in the density of EdU^+ type 1 and type 2 OLs at day 31 (Fig, S7B). This suggests that type 1 OLs precede type 2 OLs in the developmental trajectory of the OL lineage. Therefore, in the mPFC, CSS was without effect on the total density of any OL lineage cell type studied but led to a reduction in proliferative OPC density that pertained at days 16 and 31.

In the PrL or the IL specifically, as for mPFC overall, there was no effect of CSS or time on total densities of OL lineage cells (PrL: Fig. S8; IL: Fig. S9). In both subregions, total EdU^+ cell density was on average lower in CSS than CON mice, and at both time points, but statistically this was at trend level (S5B, PrL: $F(1,22) = 2.850$, $p = 0.10$; S5C, IL: $F(1,22) = 3.785$, $p = 0.06$). As for the mPFC overall, the (trend to) reduced EdU^+ cell density in CSS mice was attributable to OPCs and this co-occurred with a reduction in EdU-labelled OPCs from day 16 to day 31 (PrL: group: $p = 0.10$, time: $F(1,22) = 11.91$, $p = 0.002$; IL: group: $p = 0.11$, time: $F(1,22) = 30.00$, $p < 0.0001$), consistent with the expected OL turnover (Young et al., 2013). There was no effect of CSS on the number of cleaved caspase 3 cells, as an apoptotic marker (Fig. S10A).

3.2.2. CSS leads to decreased OPC proliferation and increased OL lineage maturation in basolateral amygdala

In BLA (Fig. 3) there was no effect of CSS or time on total OPC density (Fig. 3A). The total density of type 1 OLs was higher in CSS than CON mice at day 31 (Fig. 3A, group x time interaction: $F(1,22) = 7.248$, $p = 0.01$, Tukey's multiple comparison test: d31 CSS > CON). The total density of type 2 OLs was higher in CSS than CON mice independently of time (Fig. 3A, group: $F(1,22) = 6.177$, $p = 0.02$). CSS had no effect on the total number of proliferative cells in the BLA, whilst a decrease in the total number of proliferative cells was detected in both CSS and CON mice from day 16 to day 31 (Fig. S5D, EdU^+, time: $p = 0.02$). In OL lineage cells specifically, CSS led to a reduction in proliferative OPCs (Fig. 3B, group: $F(1,22) = 4.987$, $p = 0.04$). This co-occurred with a reduction in proliferative OPCs in both groups from day 16 to day 31 (time: $F(1,22) = 46.65$, $p < 0.0001$), a time effect that also occurred in mPFC (subregions) and is in line with the expected OL turnover (Young et al., 2013). There was no effect of CSS or time on the density of EdU^+ type 1 OLs (Fig. 3B). For EdU-labelled type 2 OLs (Fig. 3C), there was no effect of CSS, whilst their density increased in both groups from day 16 to day 31 (Fig. 3C, $EdU^+/ASPA^+$, time: $F(1,22) = 13.30$, $p = 0.001$), consistent with the expected OL turnover (Young et al., 2013). Interestingly, in both groups at day 16, most of the EdU^+ OLs belonged to type 1 OLs, and the density of EdU^+ type 1 OLs was higher than the density of EdU^+ type 2 OLs (Fig. S7C, cell type: $F(1,11) = 7.254$, $p = 0.02$). There was no difference in the density of EdU^+ type 1 and type 2 OLs at day 31 (Fig, S7D). This suggests that type 1 OLs precede type 2 OLs in the developmental trajectory of the OL lineage. Therefore, in the BLA, CSS led to an increase in total type 1 OLs by day 31, an increase in total type 2 OLs by day 16 that was maintained until day 31, and a sustained decrease in OPC proliferation by day 16 that persisted until day 31. There was no evidence that the increase in type 2 OLs in CSS

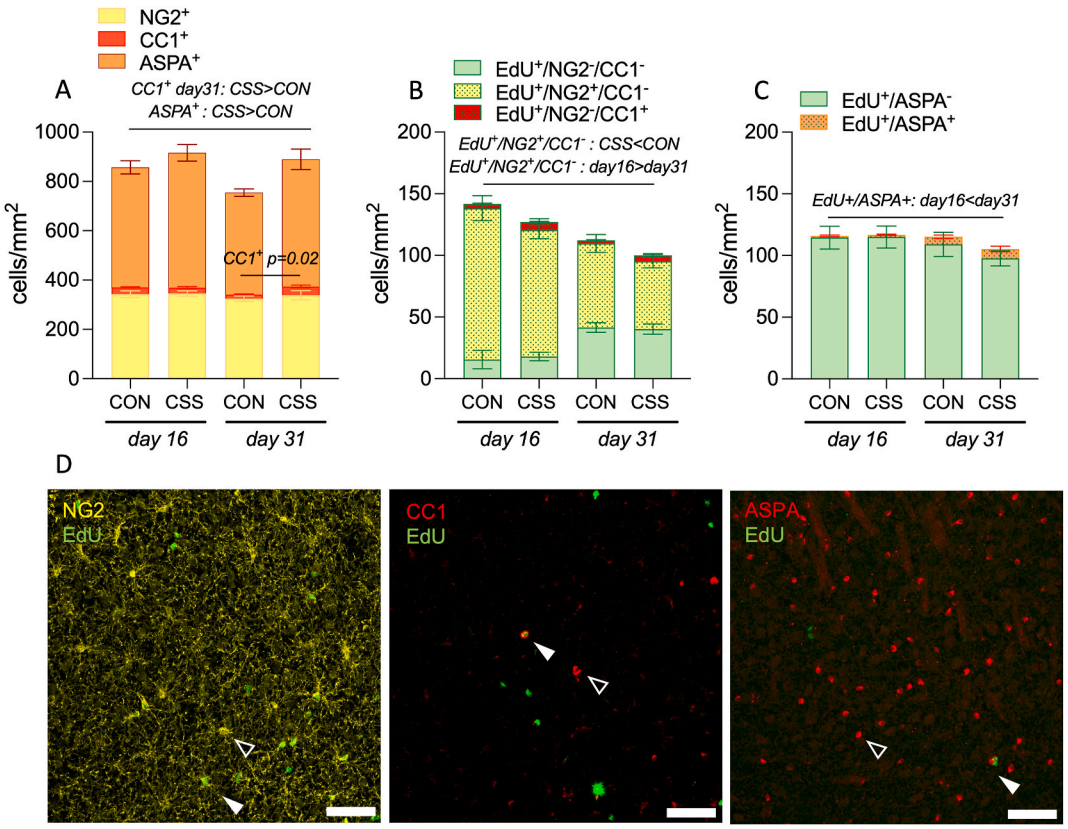

Fig. 3. Chronic social stress (CSS) reduces OPC proliferation and increases the total density of mature oligodendrocytes in basolateral amygdala. (A) Total NG2$^+$ cell density was comparable between groups and time points (2-way ANOVA, group: $p = 0.56$; time: $p = 38$; group x time interaction: $p = 0.69$). Total CC1$^+$ cell density was higher in CSS than CON mice at day 31 (2-way ANOVA, group x time interaction: $F(1,22) = 7.248$, $p = 0.01$). Total ASPA$^+$ cell density was higher in CSS than CON mice in the absence of an effect of time (2-way ANOVA, group: $F(1,22) = 6.177$, $p = 0.02$; time: $p \geq 0.13$). (B) Density of EdU$^+$/NG2$^+$/CC1$^-$ cells was lower in CSS than CON mice and decreased from day 16–31 (2-way ANOVA, group: $F(1,22) = 4.987$, $p = 0.04$; time: $F(1,22) = 46.65$, $p < 0.0001$). Density of EdU$^+$/NG2$^-$/CC1$^+$ cells was comparable between groups and time points (2-way ANOVA, group: $p \geq 0.13$; time: $p \geq 0.40$). (C) Density of EdU$^+$/ASPA$^+$ cells increased from day 16–31, without an effect of CSS (2-way ANOVA, time: $F(1,22) = 13.30$, $p = 0.001$; group: $p \geq 0.55$). Data are presented as mean ± SEM cells/mm^2, with values for each mouse being the mean of 2 sections x 2 hemispheres per mouse. (D) Representative micrographs of the OL lineage markers in basolateral amygdala (open arrows denote OL marker, closed arrow denotes OL marker and EdU$^+$). Scale bar = 50 μm. Brightness and contrast have been adjusted for display purposes.

mice was related to a reduction in apoptosis based on the number of cleaved caspase 3 cells (Fig. S10B).

3.2.3. *Unresolved identity of a proportion of EdU-positive cells*

As can be deduced from Figs. 2 and 3, in mPFC and BLA about 15% of EdU$^+$ cells at day 16 and 35% of EdU$^+$ cells at day 31 were neither NG2$^+$ nor CC1$^+$. Based on ASPA staining of adjacent brain sections, it is clear that only a small proportion of these cells could be type 2 OLs (see Figs. 2C and 3C). Our attempt to identify these cells as belonging to the OL lineage using Olig2 staining as a pan-OL marker were unsuccessful (see Materials and Methods, Fig. S3). Therefore, we focused on exclusion of other potential cell types. Microglia immunostaining was conducted with the markers Iba1 and CD68. The total density of microglia was unaffected by CSS and only a low proportion of EdU$^+$ cells was identified as microglia (Fig. S11). (In a study with BrdU and the astrocyte marker glial fibrillary acidic protein (GFAP), no BrdU$^+$ cells were astrocytes (Fig. S11)). Since the analysed brain regions are distant from the conventional regions for adult neurogenesis (e.g. (Urbán and Guillemot, 2014) and the EdU$^+$-labelled nuclei were relatively small (Fig. S12), it is unlikely that the EdU$^+$ cells of unidentified cell type belonged to the neuronal lineage. Overall, therefore, EdU$^+$ cells that were neither NG2$^+$ nor CC1$^+$ might well belong to the OL lineage, potentially at an intermediate stage of maturation.

3.3. *Chronic social stress leads to increased myelin basic protein in mPFC specifically*

Changes in the OL lineage might result in alterations in myelin content. Therefore, we investigated the effects of CSS on myelination status in mPFC and BLA using quantitative immunofluorescence for the myelin-specific marker MBP and qualitative counter-staining for the mature axon marker NF200. In mPFC (Fig. 4A), CSS resulted in increased MBP integrated density (IntDen) at day 31 (group x time interaction: $F(1,21) = 5.949$, $p = 0.02$, Tukey's multiple comparison test: d31 CSS > CON; time $p = 0.002$). When analysing the two mPFC subregions separately, effects were comparable to mPFC overall. Thus, in PrL (Fig. S13A), CSS resulted in increased MBP IntDen (group: $F(1,20) = 4.809$, $p = 0.04$), and this effect tended to be more pronounced at day 31 than day 16 (group x time: $p = 0.08$; time: $p = 0.0007$). In IL (Fig. S13B), CSS induced increased MBP IntDen at day 31 specifically (group x time: $F(1,21) = 5.582$, $p = 0.03$, Tukey's multiple comparison test day31: CSS > CON $p = 0.03$). Therefore, despite the absence of effects on type 1 or type 2 OLs in the mPFC, CSS increased the intensity of MBP immunostaining, most prominently at day 31 post-CSS onset. These findings represent a double dissociation with those observed in the BLA: That is, whereas CSS led to an increase in BLA total type 2 OLs at days 16 and 31 and type 1 OLs at day 31 (see above), there was no effect of CSS on MBP IntDen at day 16 or 31 (Fig. 4B). MBP IntDen in BLA was increased at day 31 compared with day 16 (time: $F(1,20) = 5.905$, $p = 0.02$); in addition, it is noteworthy that mean MBP IntDen

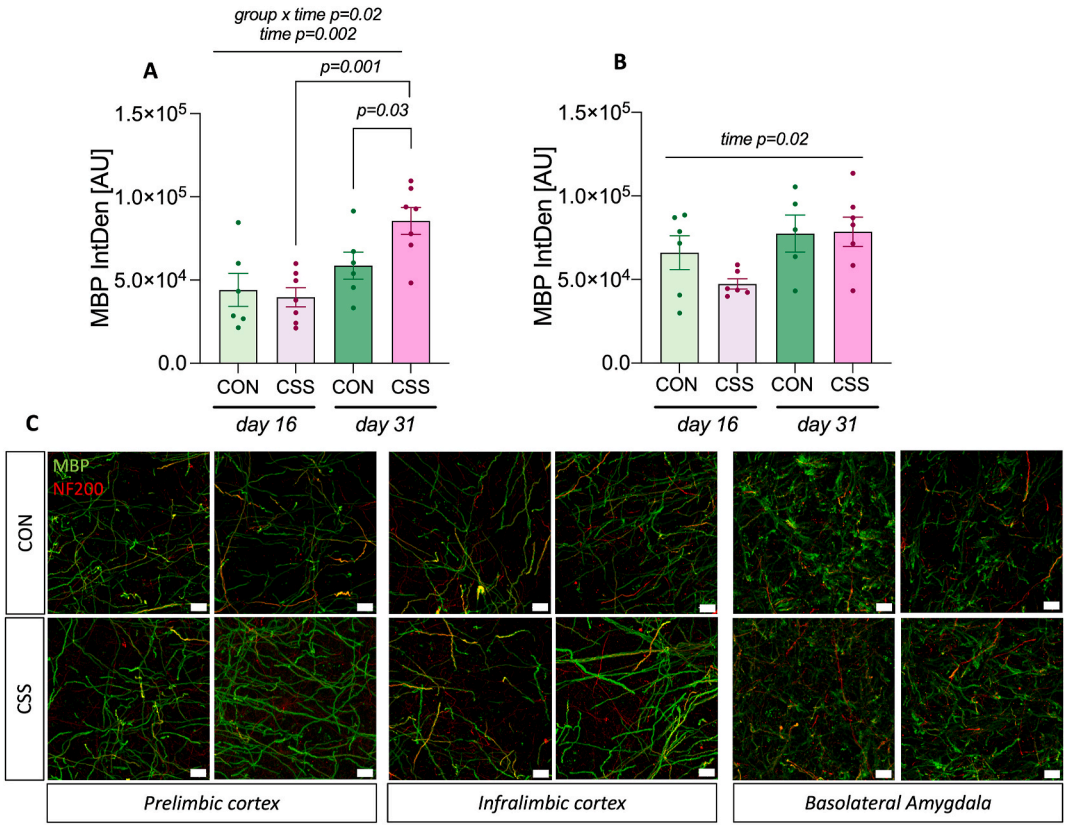

Fig. 4. Chronic social stress (CSS) leads to increased MBP signal in medial prefrontal cortex and is without effect in basolateral amygdala. (A) mPFC MBP intensity density was increased in CSS vs CON mice at day 31 (2-way ANOVA, group x time interaction: $F(1, 21) = 5.949$, $p = 0.02$; group: $p \geq 0.08$; time: $p = 0.002$). (B) BLA MBP intensity density was comparable between groups and higher at day 31 than day 16 (2-way ANOVA, group: $p \geq 0.27$; time: $F(1,20) = 5.90$, $p = 0.02$). Data are presented as mean ± SEM integrated density, with values for each mouse and brain region being the mean of 2 sections x 2 hemispheres per mouse. (C) Representative micrographs of MBP and NF200 in mPFC (prelimbic and infralimbic cortices separately) and BLA. Scale bar = 10 μm.

was relatively low in CSS mice at day 16.

3.4. Chronic social stress leads to alterations in myelin ultrastructure in mPFC specifically

The increase in MBP signal intensity in mPFC in CSS mice at day 31 could reflect CSS-induced changes in myelinated-axon density and/or myelin thickness per axon. To investigate these factors, complementary to the MBP experiment, transmission electron microscopy was conducted on mPFC and AMY samples from brains collected at day 16 in a separate cohort of CSS and CON mice (Expt 2) (Fig. 5A). In mPFC, CSS led to an increase in myelinated axon density (Fig. 5B, unpaired *t*-test, $t = 2.427$, $df = 5.833$, $p = 0.05$). The myelin g-ratio was calculated excluding the non-compacted myelin compartment and the periaxonal space: there was a tendency to a lower g-ratio (increased myelination) in CSS compared with CON mice (Fig. 5C, unpaired *t*-test $p = 0.07$), and there was an increase in myelin thickness with adjustment for axonal diameter in CSS versus CON mice (Fig. 5D, unpaired *t*-test $p = 0.01$). Importantly, the mean diameters of the axons included in the quantification were comparable between groups (Fig. 5E) and therefore unlikely to be the underlying cause of the CSS effects on myelin. Indeed, there were similar, significant positive correlations between g-ratio and axon diameter in CSS ($r = 0.51$, $p < 0.0001$) and CON mice ($r = 0.59$, $p < 0.0001$) (Fig. 5F), and also similar significant positive correlations between myelin thickness and axon diameter in CSS ($r = 0.54$, $p < 0.0001$) and CON mice ($r = 0.45$, $p < 0.0001$) (Fig. 5G).

In AMY, CSS did not influence myelinated axon density (Fig. 6A). Also, there was no effect of CSS on g-ratio (Fig. 6B), or on myelin thickness adjusted for axonal diameter (Fig. 6C). As for mPFC, also in AMY, axonal diameter was comparable between groups (Fig. 6D). There were also similar, significant positive correlations between g-ratio and axon diameter in CSS ($r = 0.57$, $p < 0.0001$) and CON mice ($r = 0.60$, $p < 0.0001$) (Fig. 6E), and also similar significant positive correlations between myelin thickness and axon diameter in CSS ($r = 0.40$, $p < 0.0001$) and CON mice ($r = 0.40$, $p < 0.0001$) (Fig. 6F).

Taken together, consistent with the MBP signal quantification readouts, CSS impacted on myelin content and ultrastructure in mPFC specifically, leading to an increase in myelin content (myelinated axon density), an increase in myelin thickness adjusted for axonal diameter, and a tendency to an increase in myelin thickness (lower g-ratio). CSS had no effect on myelin content or ultrastructure in AMY.

4. Discussion

Human MRI and post-mortem histological studies provide some evidence for changes in OL lineage and myelination status in ACC, AMY and the ACC-AMY network in patients with stress-related psychiatric disorders (Drevets, 2001; Harrison, 2002; Hughes and Shin, 2011; Kim and Whalen, 2009). These regions and this network are directly involved in the regulation of aversion processing, dysfunctions of which constitute major symptoms in stress-related disorders. Accordingly, it is important to investigate the nature and extent of effects of chronic psychosocial stress on OL lineage and myelin status in relevant animal models. In previous studies, CSS in young-adult mice was shown to lead to increased mPFC- and AMY-dependent behavioral responsiveness to aversion, increased mPFC-AMY functional connectivity, metabolite changes in mPFC and AMY, increased levels of immune-inflammation markers in mPFC and AMY, and decreased expression of OL-enriched genes in mPFC and AMY (Adamcyzk et al., 2021; Azzinnari et al., 2014; Bergamini et al., 2018; Cathomas et al., 2019; Fuertig et al., 2016;

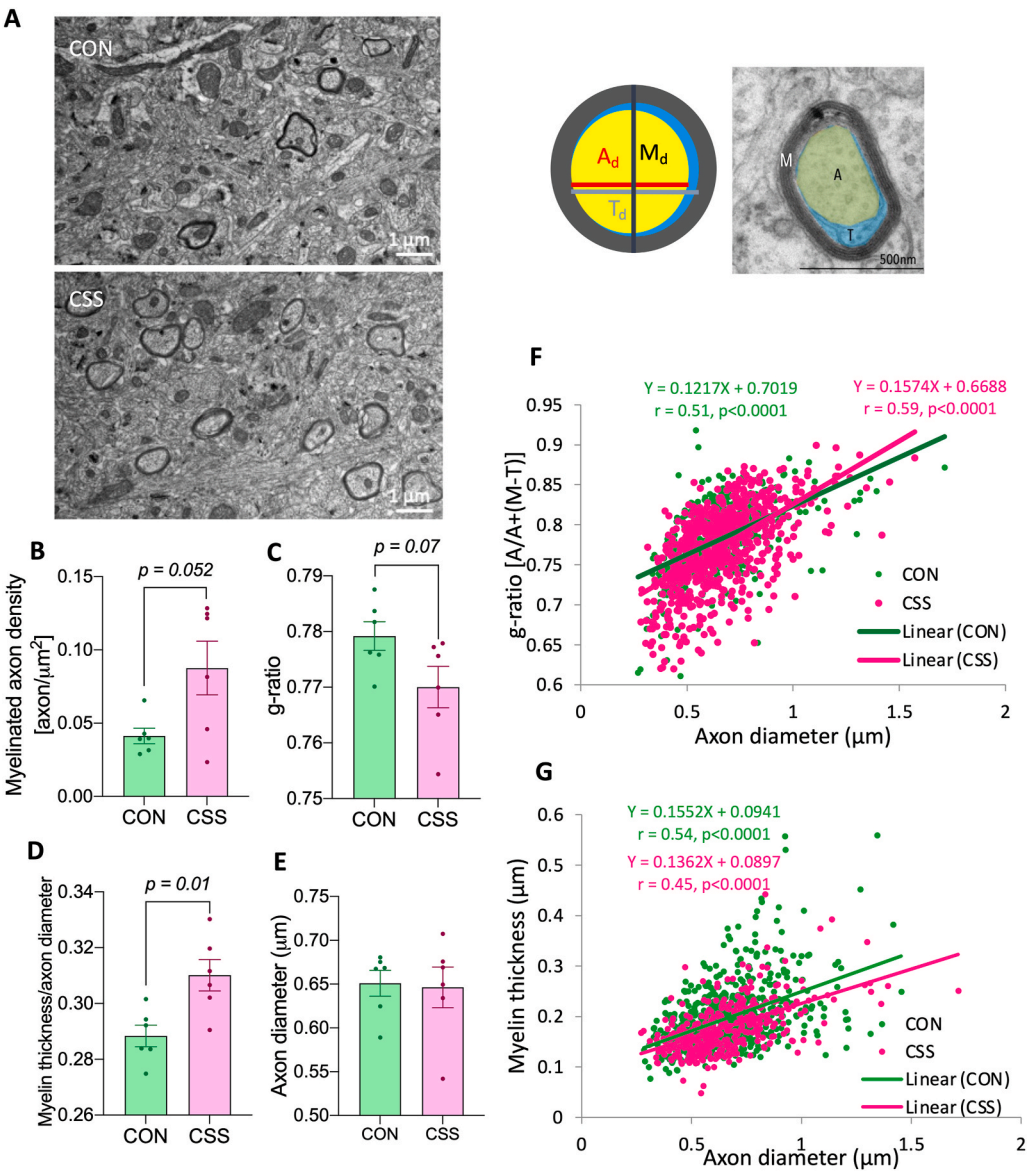

Fig. 5. Chronic social stress (CSS) leads to increased myelinated axon density and myelin thickness in the mPFC. (A) Electron micrograph of a coronal section of an axon in the mPFC of a CON mouse and a schema indicating the measurement of relevant parameters: g-ratio was calculated excluding the non-compacted myelin and the periaxonal compartment, i.e. $[A_d/A_d(M_d\text{-}T_d)]$, where A_d = axonal diameter, M_d = diameter of: axon + non-compacted myelin (and periaxonal compartment) + compacted myelin, T_d = diameter of: non-compacted myelin compartment (and periaxonal compartment) + axon. (B) Myelinated axon density was increased in CSS mice (2-tailed unpaired *t*-test with Welch's correction, t = 2.43, df = 10, p = 0.05). (C) g-ratio tended to be lower in CSS mice (2-tailed unpaired *t*-test, t = 2.029, df = 10, p = 0.07). (D) CSS led to increased myelin thickness corrected by axonal diameter (2-tailed unpaired *t*-test, t = 3.17, df = 10, p = 0.01). (E) Diameter of the analysed myelinated axons was similar in CSS and CON mice (2-tailed unpaired *t*-test, t = 0.17, df = 10, p = 0.87). (F) g-ratio was correlated positively with axon diameter in CSS and CON mice (CSS Pearson's r = 0.59, p < 0.0001; CON Pearson's, r = 0.51, p < 0.0001). The linear least squares regression equations and corresponding best-fit lines are given for CON and CSS mice separately. (G) Myelin thickness was correlated positively with axon diameter in CSS and CON mice (CSS Pearson's r = 0.45, p < 0.0001; CON Pearson's r = 0.54, p < 0.0001). Data are presented as individual values and mean ± SEM in B-E and as scatter plots in F and G.

Grandjean et al., 2016; Just et al., 2018). In the present study, we investigated to what extent CSS affects OL lineage proliferation-maturation and myelination status in mouse mPFC and AMY. Through a combination of cell fate mapping and histological approaches applied to mPFC and AMY tissues, we demonstrate that CSS affects OPC proliferation, OL-lineage cell density, MBP density and myelin thickness, and largely in a region-specific manner. A summary of the findings is given in Fig. 7A.

In the mPFC, CSS was without effect on the densities of OPCs ($NG2^+$/$CC1^-$ cells), type 1 OLs ($NG2^-/CC1^+$ cells) and type 2 OLs ($CC1^+/ASPA^+$ cells). A paradigm referred to as chronic social defeat stress (CSDS) (Golden et al., 2011) is similar to CSS but has several important differences: these include a duration of 10 rather than 15 days, and classification of mice into "susceptible" versus "resilient" based on whether they subsequently avoid or approach CD-1 mice, respectively. In one study, CSDS led to decreased mPFC OPC density in susceptible versus resilient mice at days 8 and 18 (Birey et al., 2015), and in another study it led to increased mPFC OPC density in susceptible versus control and resilient mice (Bonnefil et al., 2019). The mPFC density of mature OLs was decreased in susceptible versus control mice in the latter study (Bonnefil et al., 2019). In a study in which CSDS had a duration of 14 days, all CSDS mice subsequently avoided CD-1 mice i.e. were susceptible, and brains were collected at day 15: there was no effect of CSDS on mPFC mature OL density (Lehmann et al., 2017). In the present study, whilst CSS was without effect on the total densities of OL lineage cells in mPFC, using EdU we were able to demonstrate that proliferation of OPCs was decreased in CSS mice at days 16 and 31. The CSS-induced decrease in OPC proliferation was not sufficient to lead to a reduction in the total OPC population density.

A study that evaluated the effects of maternal separation at postnatal days 2–14 (early-life stress) on OL lineage proliferation showed that OPC proliferation was decreased at postnatal day 15; whilst total OPC density was unaffected at this time point, it was decreased in adulthood (Teissier et al., 2020). In the current study, the decrease in OPC proliferation in CSS mice co-occurred with no change in the densities of EdU^+ type 1 OLs or type 2 OLs. This can be explained by the evidence for the adult mouse that, typically, in the cortex only about 25% of newly generated pre-myelinating OLs are integrated stably into the network and the majority die within 2 days of differentiation (Hughes et al., 2018). Furthermore, the lack of a contiguous effect of decreased OPC proliferation on the total density of type 1 OLs or type 2 OLs might indicate that, in mPFC, a higher proportion of extant (non-EdU-labelled) OPCs

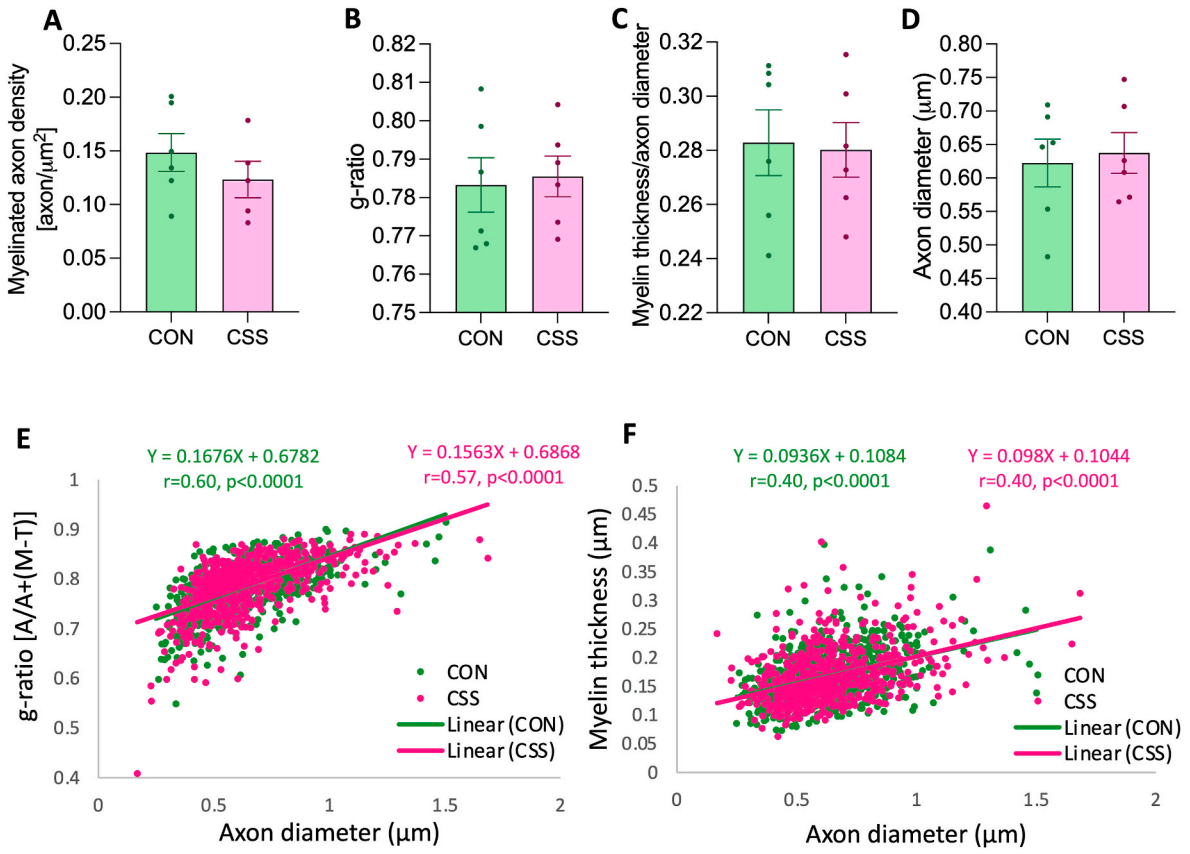

Fig. 6. Chronic social stress (CSS) is without effect on myelinated axon density and myelin thickness in the AMY. CSS and CON mice were similar in terms of: (A) Myelinated axon density ($p = 0.34$). (B) g-ratio ($p = 0.81$). (C) Myelin thickness corrected by axonal diameter ($p = 0.87$). (D) Axon diameter ($p = 0.76$). (E) g-Ratio was correlated positively with axon diameter in CSS and CON mice (CSS Pearson's $r = 0.57$, $p < 0.0001$; CON Pearson's $r = 0.60$, $p < 0.0001$). (F) Myelin thickness was correlated positively with axon diameter in CSS and CON mice (CSS Pearson's $r = 0.40$, $p < 0.0001$; CON Pearson's $r = 0.40$, $p < 0.0001$). Data are presented as individual values and mean ± SEM in A-D and as scatter plots in E and F.

matured into type 1 OLs and type 2 OLs in CSS mice than in CON mice. Using cleaved caspase 3, there was no evidence that CSS affected apoptosis. Another possibility is that lower density of EdU^+ cells in CSS compared with CON mice was due to an increased amount of DNA repair, which would temporarily block cell-cycle progression and could therefore reduce EdU incorporation (Branzei and Foiani, 2008). One way to further corroborate the reduction in cell proliferation would be to employ a marker for actively proliferating cells, such as Ki-67, in combination with EdU labelling. However, a single time-point marker to investigate this would probably identify rather few actively proliferating cells and render quantitative analysis difficult. It is also relevant that, next to their role in oligodendrogenesis, some OPCs have other functions in the adult brain, including immunomodulation and neuromodulation (Akay et al., 2021). One limitation of this study is that despite having employed a comprehensive set of OL lineage markers, we did not have an antibody for Olig2 that labelled all $NG2^+$, $CC1^+$ or $ASPA^+$ cells, and would therefore serve as a pan-OL marker, to investigate whether the relatively high number of EdU^+ cells that did not express CC1, NG2 or ASPA belonged to the OL lineage. We do provide evidence that only a small number of these cells are microglia or astrocytes. It is possible that the non-identified EdU^+ cells were of the OL lineage in a state of maturation between OPCs and OLs. To clarify this issue, a future study would need to identify a suitable pan-OL marker, and possibly also employ OL markers that specifically label pre-myelinating and newly forming OLs, such as breast carcinoma amplified sequence 1 (BCAS1) and ectonucleotide pyrophosphatase/phosphodiesterase 6 (Enpp6) (Fard et al., 2017; Xiao et al., 2016).

Perhaps related to this apparent shift in OL lineage proliferation-maturation, clear evidence for increased myelin content and thickness in the mPFC of CSS compared with CON mice was obtained with both immunofluorescence- and TEM-based readouts, which were carried out in two separate CSS-CON cohorts. This pro-myelination effect of CSS was apparent at days 16 and 31 and, according to quantitative immunofluorescence for MBP, was more prominent at the latter time point, consistent with a sustained and cumulative effect. This mPFC finding differs from those of studies conducted with CSDS, and the latter also differ from each other to some extent: With 14-day CSDS (without susceptibility subgrouping) and collection of brains at day 15, CSDS led to decreased mPFC myelin fiber density (Lehmann et al., 2017). Ten-day CSDS was without effect on percentage of mPFC covered by MBP area but did lead to decreased mPFC myelin thickness in susceptible mice specifically (Bonnefil et al., 2019). Also using 10-day CSDS, there was no change in myelin thickness in susceptible mice and an increase in resilient mice, relative to controls (Laine et al., 2018). These inter-study differences in the observed effects of chronic social stress on mPFC myelination status could well be attributable to differences in the protocol duration, duration of daily attacks, whether or not the teeth of CD-1 mice are trimmed to avoid wounding, and whether or not mice are sub-grouped according to passive avoidance of the aggressor mouse strain.

Therefore, CSS led to a decrease in OPC proliferation and a sustained increase in myelination, in mPFC. Recently, it was reported that contextual aversion learning in relation to high-intensity foot-shock is associated with an immediate increase in proliferation of OPCs (day 1) which mature into OLs (day 30) as well as with increased myelination (day 30), in mPFC (both PrL and IL) (Pan et al., 2020). The same study demonstrated that transgenic blocking of new OL formation in mPFC after contextual aversion learning prevented the recall, and presumably

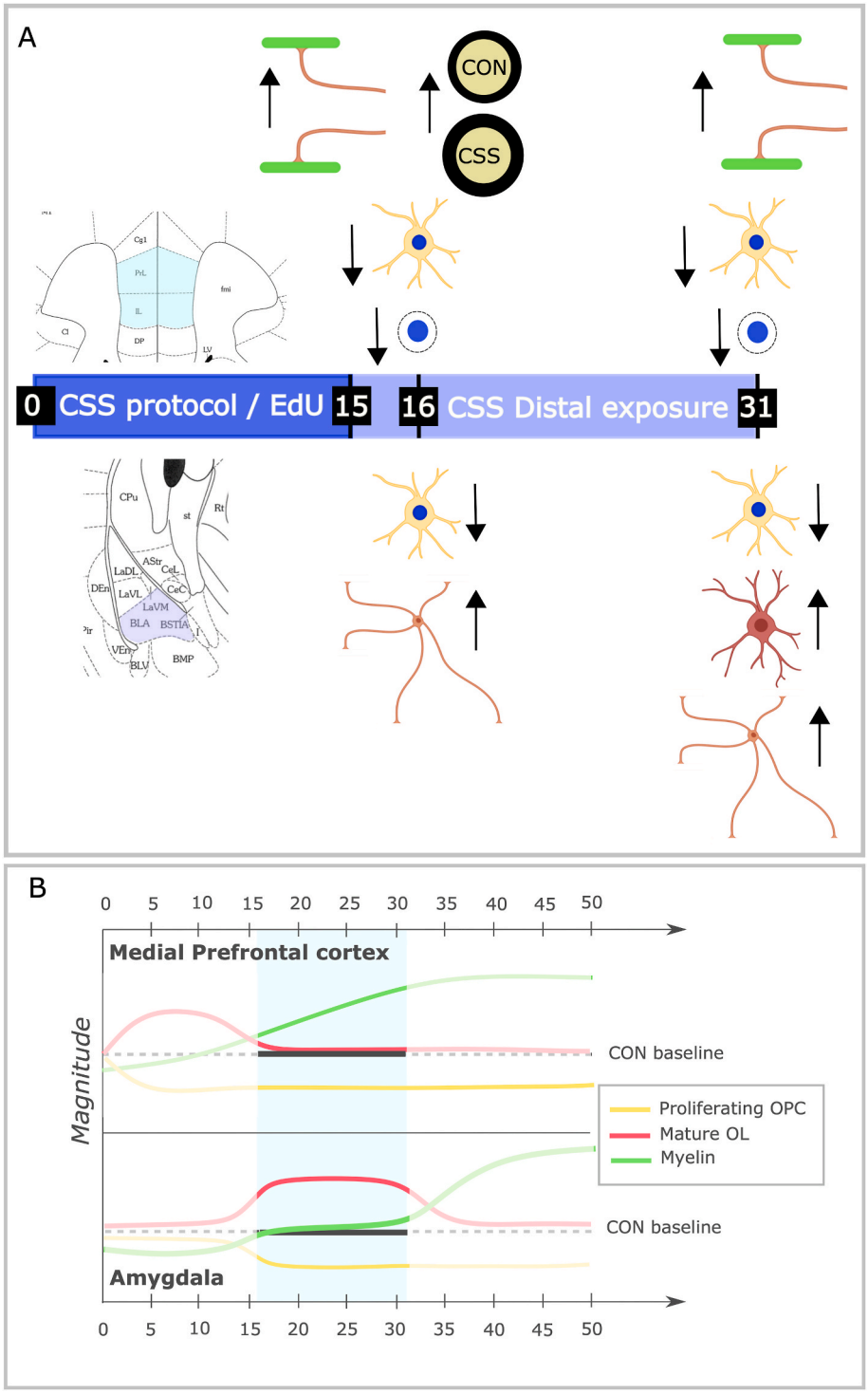

Fig. 7. Double dissociation of CSS effects in mPFC and AMY: summary of findings and explanatory hypothesis. (A) Summary of findings. The upper part of the figure depicts the mPFC and the lower part the BLA/AMY. In mPFC, CSS led to a decrease in overall cell proliferation attributable to OPCs, at days 16 and 31. CSS led to increases in MBP density at days 16 and 31 and myelin thickness at day 16. In BLA, CSS led to increases in densities of type 1 OLs at day 31 and type 2 OLs at days 16 and 31. CSS led to a decrease in proliferative OPCs at days 16 and 31. CSS was without effects on MBP density or myelin thickness at days 16 and 31. Figure created with BioRender.com. (B) Model of the actual and hypothesized temporal sequences of events in mPFC and AMY. The x-axis depicts time in days from the start of the CSS protocol (day 0) to day 45, and the y-axis depicts the relative quantities of OL lineage cells and myelin across this time period. The light blue area depicts days 16 and 31, the time points at which experimental data were collected. The black line (solid, dashed) depicts the control (CON) condition. The data points prior to day 16 and after day 31 depict data points consistent with the hypothesis that the current findings do not represent a double dissociation between mPFC and AMY, but rather a shift in their temporal responses to CSS in terms of OL lineage status and myelination status. (For interpretation of the references to colour in this figure legend, the reader is referred to the Web version of this article.)

the storage, of aversion memory, consistent with a critical role for *de novo* mPFC myelination synthesis in storing adaptive long-term aversion memories (Pan et al., 2020). That CSS also induces increased mPFC myelination, as well as excessive, i.e. maladaptive, contextual and discrete conditioned-stimulus aversion learning and memory (Adamcyzk et al., 2021; Azzinnari et al., 2014; Cathomas et al., 2019; Fuertig et al., 2016), suggests that increased mPFC myelination can shift from adaptive to maladaptive as environments shift from acutely to chronically aversive.

To our knowledge, this is the first mouse study to investigate chronic social stress effects on OL lineage-marker density in AMY. In the BLA, CSS led to increases in the densities of type 1 OLs at day 31 and of type 2 OLs at days 16 and 31. This co-occurred with a decrease in OPC proliferation in CSS mice at both days 16 and 31, whilst there was no contiguous effect on the densities of EdU^{+} type 1 OLs or type 2 OLs. Taken together, these BLA findings suggest that a higher proportion and absolute number of extant OPCs matured into OLs in CSS mice than was the case in CON mice. Despite the increase in type 2 OL density in CSS mice, there was no contiguous CSS effect on MBP integrated density in the BLA of these same mice. Furthermore, in Expt 2, there was no CSS effect on myelin thickness in AMY, as measured at day 16.

Therefore, whilst there was a common and sustained inhibitory

effect of CSS on OPC proliferation in both mPFC and BLA/AMY, the other CSS effects observed were region-specific. Indeed, that CSS was without effect on OL-cell densities and increased MBP intensity/myelin thickness in mPFC whilst it increased OL-cell densities and was without effect on MBP intensity/myelin thickness in BLA/AMY, constitutes, *prima facie* at least, a double dissociation. This might reflect basic differences in OL lineage and myelination between cortical and subcortical regions. Indeed, even within the cortex, myelination is heterogeneous, with respect to myelin abundance and axonal distribution, which vary according to cortical region and neuronal type (Call and Bergles, 2021; Yang et al., 2021). However, it is also possible that the timing of the CSS response sequence is region-specific. Some evidence for differential responsiveness of mPFC and BLA OL lineages to aversion is provided by a study of contextual aversion learning: newly formed OLs were already detectable at 7 days post-aversion conditioning in mPFC, whilst in BLA such cells started to be observable at 14 days post-aversion learning (Pan et al., 2020). Extrapolating from this, it is possible that, relative to that of the mPFC, the AMY response to CSS is also delayed, and that at a time point beyond day 31 there would be an increase in MBP intensity and myelin thickness in AMY. This hypothesis is illustrated in Fig. 7B and remains to be investigated.

In a previous, hypothesis-free study that deployed region-specific tissue RNA sequencing (Cathomas et al., 2019), CSS led at day 16 to down-regulation of expression of 20 and 34 oligodendrocyte-enriched genes in mPFC and AMY (BLA and central nucleus), respectively, with a high degree of overlap in gene identity between the two regions. Identity of cell type-specific gene enrichment was based on a transcriptome database for mouse forebrain tissue (Cahoy et al., 2008): approximately half of the genes downregulated by CSS were classified as "enriched in OLs compared to OPCs" (Cahoy et al., 2008), whereas none of the down-regulated genes were classified as "enriched in OPCs" (Cahoy et al., 2008). Integrating these day 16 transcriptome study findings and the current study day 16 findings of unchanged total OL lineage density in mPFC and increased total OL lineage density in AMY, the evidence indicates that the CSS-induced decrease in expression of OL-enriched genes in mPFC and BLA reflects a decrease in expression of certain genes in extant OLs. Whether or not there is a causal association in AMY at day 16 between the decrease in gene expression in extant OLs (Cathomas et al., 2019) and the increase in OL density, remains to be investigated. The absence of a CSS effect on OPC-enriched transcripts in mPFC and AMY (Cathomas et al., 2019) is consistent with the stable density of total OPCs observed in mPFC and AMY at day 16 in the present study. Furthermore, with respect to myelination, in the mPFC, the transcript level of *Mbp* was not changed by CSS and no CSS effect on mPFC MBP was observed at day 16 in the present study. In the AMY, whereas the transcripts for *Mbp* and *Plp1* were downregulated in CSS mice, there was no corresponding CSS effect at the protein level (Cathomas et al., 2019), and no CSS effect on AMY MBP was observed at day 16 in the present study.

Clearly, mouse studies investigating effects of chronic social stress on mPFC OL lineage and myelin content have yielded heterogeneous findings to date. This could well be due to the specifics of the daily procedure, the total duration of the social aversion procedure, the timing of brain collection, and whether additional manipulations were included, most notably behavioural testing. Regarding the specifics of the daily procedure, one difference is likely to be bite wounds and their consequences. In our CSS protocol, we minimize bite wounds by trimming the teeth of the CD-1 mice, whilst this is not the case for the standard CSDS protocol (Golden et al., 2011). Bite wounds induce peripheral inflammatory processes and, in turn, chronic peripheral inflammation can lead to microglia-mediated inflammatory responses in the central nervous system (Süß et al., 2020). Microglia are intimately involved in the regulation of OL lineage and myelin function (Hughes and Appel, 2020; Lloyd et al., 2017; Stadelmann et al., 2019). Psychological stress activates the immune-inflammatory system via the sympathetic autonomic nervous system and its release of catecholamines, which in turn are bound by adrenergic receptors expressed by immune cells, most notably macrophages (Miller et al., 2009). There is substantial evidence that stress-related psychiatric disorders often present with increased peripheral and central indices of chronic, low-level inflammation (Fleshner et al., 2017; Rohleder, 2014). It is therefore important that stress-based animal models that aim to increase understanding of the pathophysiology of these disorders do, indeed, include chronic, low-level inflammation induced by social subordination stress. At the same time, it is essential to minimize the confounding effects of marked immune-inflammatory activation induced by physical (bite) wounding. In our CSS protocol with minimizing of bite wounding by trimming the teeth of the CD-1 mice, mice obtain on average two small surface wounds across the 15-day period, as in the present study. In CSS mice compared with CON mice, we observe moderate, consistent increases in spleen myeloid cells (e.g. granulocytes, inflammatory monocytes) and moderately higher blood levels of pro-inflammatory cytokines and kynurenine metabolites (Azzinnari et al., 2014; Bergamini et al., 2018; Fuertig et al., 2016). In the brain, CSS has no effect on whole-brain microglia, macrophages or lymphocytes (Bergamini et al., 2018); region-specific activation of microglia in terms of Iba1 immunoreactivity is observed in sub-cortical regions including AMY, but not in mPFC (Bergamini et al., 2018; Cathomas et al., 2019). To the best of our knowledge, teeth trimming of CD-1 mice is not used in CSDS protocols (e.g. (Golden et al., 2011)). The procedure of repeated social defeat stress (RSDS), comprising 2 h physical exposure to a CD-1 mouse on each of 6 days, led to whole-brain activation of microglia and even to monocyte trafficking from periphery to brain (Wohleb et al., 2012, 2014). It is possible that the profound activation of central inflammatory processes by RSDS – much greater than that caused by CSS - is attributable to high levels of wounding and, whilst RSDS is unusual in the long duration of each bout of physical attack, these differences in the extent of brain immune-inflammatory activation testify to the importance of minimizing physical wounding with respect to model validity. In summary, some reported effects of CSDS/RSDS on OLs and myelin could be due to physical wounding; it is essential to minimize any such effects in order to maximize the translational relevance of the observed effects, including those on the OL lineage and myelination, to human psychosocial stress-related psychiatric disorders.

Concerning the latter, to-date a small number of histological studies have investigated OL lineage cells specifically (in contrast to glia in general) in tissue from MDD patients and control subjects and, to our knowledge, no data are available for GAD or PTSD. In the AMY, the density of OL lineage cells, identified using Nissl staining, was decreased in MDD compared with control subjects (Hamidi et al., 2004). In the frontal region, including ACC, one study identified a reduction of $NG2^+$ cell density in MDD patients compared to controls (Birey et al., 2015). In the white matter adjacent to the pregenual ACC, the density of cells positive for the OL lineage-cell marker Olig1 in the nuclear compartment was increased in MDD, but the density of fibers expressing MBP was unchanged (Mosebach et al., 2013). In another study (Lutz et al., 2017), there was no change in ACC OL lineage cell density, myelin content or axonal diameter in MDD patients who committed suicide compared with controls; however, MDD patients who committed suicide and had experienced early-life abuse displayed significant reduction in each of these parameters (Lutz et al., 2017). Clearly, coherence between the findings of the current study and studies of MDD post-mortem brain tissue is limited. However, it is important to emphasize that human samples are derived from patients with varying durations of stress-related psychiatric disorder; to address the possibility that changes in the OL lineage and myelination in ACC and AMY occur early in the human disorder specifically, and that these might be similar to those induced by CSS in the mouse brain, it will be essential to identify appropriate translational biomarkers.

Whilst it is beyond the scope of the present study, it is important to mention the mechanisms which mediate chronic stress effects on the OL lineage and myelination. It is noteworthy that CSS mice display a

number of changes in external glands and organs, including increased weight of the adrenal glands and the spleen (Azzinnari et al., 2014; Bergamini et al., 2018). Accordingly, it is possible that changes in circulating levels of specific hormones, cytokines and chemokines could lead to changes in their brain levels and contribute to the CSS effects on the OL lineage and/or myelination observed in the present study (see above). Concerning increased levels of corticosterone, which the increase in adrenal gland weight indicates to occur at some point during CSS, it has been reported that this hormone does indeed influence oligodendrogenesis, at least in hippocampus (Chetty et al., 2014; Treccani et al., 2021).

5. Conclusion

In summary, the present study provides evidence for mice that chronic social stress in young adulthood leads to changes in the density and proliferation-maturation of OL lineage cells in the mPFC and AMY, including decreased OPC proliferation in both regions and increased densities of type 1 and type OLs in AMY. Furthermore, CSS led to substantial and sustained increases in MBP density and myelin thickness in the mPFC specifically and was without effect on myelination in the AMY within the study period. Whilst the limited agreement of the current findings with some previous mouse studies, and indeed the limited agreement of the latter with each other, demonstrates the need for further investigation before drawing firm conclusions regarding the definitive effects of chronic stressors on OL lineage and myelination status, the present data certainly do constitute definitive evidence that mPFC and AMY OL lineage cells and, in the case of mPFC, their myelination activity, are sensitive to chronic psychosocial aversion. Accordingly, integrated animal model and human studies will be required to elucidate the relevance of these changes to the pathophysiology and treatment of stress-related psychiatric disorders.

Funding

This research was funded by the Swiss National Science Foundation (Grant No. 31NE30_189481, in the ERA-NET NEURON Joint Transnational Research Project consortium “MoodMarker”) and a pilot grant from the Oxford-McGill-Zurich Neuroscience Collaboration.

CRediT authorship contribution statement

Giulia Poggi: Conceptualization, Validation, Formal analysis, Investigation, Writing – original draft, Writing – review & editing, Visualization, Supervision, Project administration. **Jamie Albiez:** Formal analysis, Investigation. **Christopher R. Pryce:** Conceptualization, Validation, Resources, Writing – review & editing, Supervision, Project administration, Funding acquisition.

Declaration of competing interest

The authors declare no conflict of interest.

Acknowledgments

We are grateful to Björn Henz and Alex Osei for animal care, to the Center for Microscopy and Image Analysis, University of Zurich, for assistance and support.

Appendix A. Supplementary data

Supplementary data to this article can be found online at https://doi.org/10.1016/j.ynstr.2022.100451.

References

Adamcyzk, I., Kúkeľová, D., Just, S., Giovannini, R., Sigrist, H., Amport, R., Cuomo-Haymour, N., Poggi, G., Pryce, C.R., 2021. Somatostatin receptor 4 agonism normalizes stress-related excessive amygdala glutamate release and Pavlovian aversion learning and memory in rodents. Biol. Psychiatry Glob. Open Sci. https://doi.org/10.1016/j.bpsgos.2021.11.006.

Akay, L.A., Effenberger, A.H., Tsai, L.H., 2021. Cell of all trades: oligodendrocyte precursor cells in synaptic, vascular, and immune function. Genes Dev. 35, 180–198. https://doi.org/10.1101/GAD.344218.120.

Azzinnari, D., Sigrist, H., Staehli, S., Palme, R., Hildebrandt, T., Leparc, G., Hengerer, B., Seifritz, E., Pryce, C.R., 2014. Mouse social stress induces increased fear conditioning, helplessness and fatigue to physical challenge together with markers of altered immune and dopamine function. Neuropharmacology 85, 328–341. https://doi.org/10.1016/j.neuropharm.2014.05.039.

Bergamini, G., Mechtersheimer, J., Azzinnari, D., Sigrist, H., Buerge, M., Dallmann, R., Freije, R., Kouraki, A., Opacka-Juffry, J., Seifritz, E., Ferger, B., Suter, T., Pryce, C.R., 2018. Chronic social stress induces peripheral and central immune activation, blunted mesolimbic dopamine function, and reduced reward-directed behaviour in mice. Neurobiol. Stress 8, 42–56. https://doi.org/10.1016/j.ynstr.2018.01.004.

Bergles, D.E., Richardson, W.D., 2016. Oligodendrocyte development and plasticity. Cold Spring Harbor Perspect. Biol. 8, 1–27. https://doi.org/10.1101/cshperspect.a020453.

Bierer, L.M., Ivanov, I., Carpenter, D.M., Wong, E.W., Golier, J.A., Tang, C.Y., Yehuda, R., 2015. White matter abnormalities in Gulf War veterans with posttraumatic stress disorder: a pilot study. Psychoneuroendocrinology 51, 567–576. https://doi.org/10.1016/j.psyneuen.2014.11.007.

Birey, F., Kloc, M., Chavali, M., Hussein, I., Wilson, M., Christoffel, D.J., Chen, T., Frohman, M.A., Robinson, J.K., Russo, S.J., Maffei, A., Aguirre, A., 2015. Genetic and stress-induced loss of NG2 glia triggers emergence of depressive-like behaviors through reduced secretion of FGF2. Neuron 88, 941–956. https://doi.org/10.1016/j.neuron.2015.10.046.

Bonnefil, V., Dietz, K., Amatruda, M., Wentling, M., Aubry, A.V., Dupree, J.L., Temple, G., Park, H.-J.J., Burghardt, N.S., Casaccia, P., Liu, J., 2019. Region-specific myelin differences define behavioral consequences of chronic social defeat stress in mice. Elife 8, 1–13. https://doi.org/10.7554/eLife.40855.

Branzei, D., Foiani, M., 2008. Regulation of DNA repair throughout the cell cycle. Nat. Rev. Mol. Cell Biol. 9, 297–308. https://doi.org/10.1038/nrm2351.

Cahoy, J.D., Emery, B., Kaushal, A., Foo, L.C., Zamanian, J.L., Christopherson, K.S., Xing, Y., Lubischer, J.L., Krieg, P.A., Krupenko, S.A., Thompson, W.J., Barres, B.A., 2008. A transcriptome database for astrocytes, neurons, and oligodendrocytes: a new resource for understanding brain development and function. J. Neurosci. 28, 264–278. https://doi.org/10.1523/JNEUROSCI.4178-07.2008.

Call, C.L., Bergles, D.E., 2021. Cortical neurons exhibit diverse myelination patterns that scale between mouse brain regions and regenerate after demyelination. Nat. Commun. 12 https://doi.org/10.1038/s41467-021-25035-2.

Cathomas, F., Azzinnari, D., Bergamini, G., Sigrist, H., Buerge, M., Hoop, V., Wicki, B., Goetze, L., Soares, S., Kukelova, D., Seifritz, E., Goebbels, S., Nave, K.-A.A., Ghandour, M.S., Seoighe, C., Hildebrandt, T., Leparc, G., Klein, H., Stupka, E., Hengerer, B., Pryce, C.R., 2019. Oligodendrocyte gene expression is reduced by and influences effects of chronic social stress in mice. Gene Brain Behav. 18, e12475 https://doi.org/10.1111/gbb.12475.

Chetty, S., Friedman, A.R., Taravosh-Lahn, K., Kirby, E.D., Mirescu, C., Guo, F., Krupik, D., Nicholas, A., Geraghty, A.C., Krishnamurthy, A., Tsai, M.-K.K., Covarrubias, D., Wong, A.T., Francis, D.D., Sapolsky, R.M., Palmer, T.D., Pleasure, D., Kaufer, D., 2014. Stress and glucocorticoids promote oligodendrogenesis in the adult hippocampus. Mol. Psychiatr. 19, 1275–1283. https://doi.org/10.1038/mp.2013.190.

Dimou, L., Gallo, V., 2015. NG2-glia and their functions in the central nervous system. Glia 63, 1429–1451. https://doi.org/10.1002/glia.22859.

Drevets, W.C., 2001. Neuroimaging and neuropathological studies of depression: implications for the cognitive-emotional features of mood disorders. Curr. Opin. Neurobiol. 11, 240–249. https://doi.org/10.1016/S0959-4388(00)00203-8.

Fard, M.K., Van der Meer, F., Sánchez, P., Cantuti-Castelvetri, L., Mandad, S., Jäkel, S., Fornasiero, E.F., Schmitt, S., Ehrlich, M., Starost, L., Kuhlmann, T., Sergiou, C., Schultz, V., Wrzos, C., Brück, W., Urlaub, H., Dimou, L., Stadelmann, C., Simons, M., 2017. BCAS1 expression defines a population of early myelinating oligodendrocytes in multiple sclerosis lesions. Sci. Transl. Med. 9, 1–13. https://doi.org/10.1126/scitranslmed.aam7816.

Fields, R.D., 2015. A new mechanism of nervous system plasticity: activity-dependent myelination. Nat. Rev. Neurosci. 16, 756–767. https://doi.org/10.1038/nrn4023.

Fields, R.D., 2008. White matter in learning, cognition and psychiatric disorders. Trends Neurosci. 31, 361–370. https://doi.org/10.1016/j.tins.2008.04.001.

Fleshner, M., Frank, M., Maier, S.F., 2017. Danger signals and inflammasomes: stress-evoked sterile inflammation in mood disorders. Neuropsychopharmacology 42, 36–45. https://doi.org/10.1038/npp.2016.125.

Friedman, M.J., Resick, P.A., Bryant, R.A., Strain, J., Horowitz, M., Spiegel, D., 2011. Classification of trauma and stressor-related disorders in DSM-5. Depress. Anxiety 28, 737–749. https://doi.org/10.1002/da.20845.

Fuertig, R., Azzinnari, D., Bergamini, G., Cathomas, F., Sigrist, H., Seifritz, E., Vavassori, S., Luippold, A., Hengerer, B., Ceci, A., Pryce, C.R., Staehli, S., Palme, R., Hildebrandt, T., Leparc, G., Hengerer, B., Seifritz, E., Pryce, C.R., 2016. Mouse chronic social stress increases blood and brain kynurenine pathway activity and fear behaviour: both effects are reversed by inhibition of indoleamine 2,3-dioxygenase. Brain Behav. Immun. 54, 59–72. https://doi.org/10.1016/j.bbi.2015.12.020.

Gibson, E.M., Purger, D., Mount, C.W., Goldstein, A.K., Lin, G.L., Wood, L.S., Inema, I., Miller, S.E., Bieri, G., Zuchero, J.B., Barres, B. a, Woo, P.J., Vogel, H., Monje, M., 2014. Neuronal activity promotes oligodendrogenesis and adaptive myelination in the mammalian brain. Science 344, 1252304. https://doi.org/10.1126/science.1252304.

Golden, S.A., Covington, H.E., Berton, O., Russo, S.J., 2011. A standardized protocol for repeated social defeat stress in mice. Nat. Protoc. 6, 1183–1191. https://doi.org/10.1038/nprot.2011.361.

Grandjean, J., Azzinnari, D., Seuwen, A., Sigrist, H., Seifritz, E., Pryce, C.R., Rudin, M., 2016. Chronic psychosocial stress in mice leads to changes in brain functional connectivity and metabolite levels comparable to human depression. Neuroimage 142, 544–552. https://doi.org/10.1016/j.neuroimage.2016.08.013.

Guadagno, A., Kang, M.S., Devenyi, G.A., Mathieu, A.P., Rosa-Neto, P., Chakravarty, M., Walker, C.D., 2018. Reduced resting-state functional connectivity of the basolateral amygdala to the medial prefrontal cortex in preweaning rats exposed to chronic early-life stress. Brain Struct. Funct. 223, 3711–3729. https://doi.org/10.1007/s00429-018-1720-3.

Guilloux, J.P., Douillard-Guilloux, G., Kota, R., Wang, X., Gardier, A.M., Martinowich, K., Tseng, G.C., Lewis, D.A., Sibille, E., 2012. Molecular evidence for BDNF-and GABA-related dysfunctions in the amygdala of female subjects with major depression. Mol. Psychiatr. 17, 1130–1142. https://doi.org/10.1038/mp.2011.113.

Hamidi, M., Drevets, W.C., Price, J.L., 2004. Glial reduction in amygdala in major depressive disorder is due to oligodendrocytes. Biol. Psychiatr. 55, 563–569. https://doi.org/10.1016/j.biopsych.2003.11.006.

Harrison, P.J., 2002. The neuropathology of primary mood disorder. Brain 125, 1428–1449. https://doi.org/10.1093/brain/awf149.

Hemanth Kumar, B.S., Mishra, S.K., Trivedi, R., Singh, S., Rana, P., Khushu, S., 2014. Demyelinating evidences in CMS rat model of depression: a DTI study at 7T. Neuroscience 275, 12–21. https://doi.org/10.1016/j.neuroscience.2014.05.037.

Hill, R.A., Nishiyama, A., 2014. NG2 cells (polydendrocytes): listeners to the neural network with diverse properties. Glia 62, 1195–1210. https://doi.org/10.1002/glia.22664.

Hirrlinger, J., Nave, K.A., 2014. Adapting brain metabolism to myelination and long-range signal transduction. Glia 62, 1749–1761. https://doi.org/10.1002/glia.22737.

Huang, P., Dong, Z., Huang, W., Zhou, C., Zhong, W., Hu, P., Wen, G., Sun, X., Hua, H., Cao, H., Gao, L., Lv, Z., 2017. Voluntary wheel running ameliorates depression-like behaviors and brain blood oxygen level-dependent signals in chronic unpredictable mild stress mice. Behav. Brain Res. 330, 17–24. https://doi.org/10.1016/j.bbr.2017.05.032.

Hughes, A.N., Appel, B., 2020. Microglia phagocytose myelin sheaths to modify developmental myelination. Nat. Neurosci. 23, 1055–1066. https://doi.org/10.1038/s41593-020-0654-2.

Hughes, E.G., Orthmann-Murphy, J.L., Langseth, A.J., Bergles, D.E., 2018. Myelin remodeling through experience-dependent oligodendrogenesis in the adult somatosensory cortex. Nat. Neurosci. 21, 696–706. https://doi.org/10.1038/s41593-018-0121-5.

Hughes, E.G., Stockton, M.E., 2021. Premyelinating oligodendrocytes: mechanisms underlying cell survival and integration. Front. Cell Dev. Biol. 9, 1–17. https://doi.org/10.3389/fcell.2021.714169.

Hughes, K.C., Shin, L.M., 2011. Functional neuroimaging studies of post-traumatic stress disorder. Expert Rev. Neurother. 11, 275–285. https://doi.org/10.1586/ern.10.198.

Janak, P.H., Tye, K.M., 2015. From circuits to behaviour in the amygdala. Nature 517, 284–292. https://doi.org/10.1038/nature14188.

Just, S., Chenard, B.L., Ceci, A., Strassmaier, T., Chong, J.A., Blair, N.T., Gallaschun, R.J., Del Camino, D., Cantin, S., D'Amours, M., Eickmeier, C., Fanger, C.M., Hecker, C., Hessler, D.P., Hengerer, B., Kroker, K.S., Malekiani, S., Mihalek, R., McLaughlin, J., Rast, G., Witek, J., Sauer, A., Pryce, C.R., Moran, M.M., 2018. Treatment with HC-070, a potent inhibitor of TRPC4 and TRPC5, leads to anxiolytic and antidepressant effects in mice. PLoS One 13, e0191225. https://doi.org/10.1371/journal.pone.0191225.

Kato, D., Wake, H., 2021. Myelin plasticity modulates neural circuitry required for learning and behavior. Neurosci. Res. https://doi.org/10.1016/j.neures.2020.12.005.

Kim, M.J., Whalen, P.J., 2009. The structural integrity of an amygdala-prefrontal pathway predicts trait anxiety. J. Neurosci. 29, 11614–11618. https://doi.org/10.1523/JNEUROSCI.2335-09.2009.

Laine, M.A., Sokolowska, E., Dudek, M., Callan, S.A., Hyytiä, P., Hovatta, I., 2017. Brain activation induced by chronic psychosocial stress in mice. Sci. Rep. 7, 1–11. https://doi.org/10.1038/s41598-017-15422-5.

Laine, M.A., Trontti, K., Misiewicz, Z., Sokolowska, E., Kulesskaya, N., Heikkinen, A., Saarnio, S., Balcells, I., Ameslon, P., Greco, D., Mattila, P., Ellonen, P., Paulin, L., Auvinen, P., Jokitalo, E., Hovatta, I., 2018. Genetic control of myelin plasticity after chronic psychosocial stress. eneuro 5. https://doi.org/10.1523/ENEURO.0166-18.2018, 2018, ENEURO.0166-18.

Laubach, M., Amarante, L.M., Swanson, K., White, S.R., 2018. What, if anything, is rodent prefrontal cortex? eneuro 5. https://doi.org/10.1523/ENEURO.0315-18.2018, 2018, ENEURO.0315-18.

Lehmann, M.L., Weigel, T.K., Elkahloun, A.G., Herkenham, M., 2017. Chronic social defeat reduces myelination in the mouse medial prefrontal cortex. Sci. Rep. 7, 1–13. https://doi.org/10.1038/srep46548.

Liu, J., Dietz, K., DeLoyht, J.M., Pedre, X., Kelkar, D., Kaur, J., Vialou, V., Lobo, M.K., Dietz, D.M., Nestler, E.J., Dupree, J., Casaccia, P., 2012. Impaired adult myelination in the prefrontal cortex of socially isolated mice. Nat. Neurosci. 15, 1621–1623. https://doi.org/10.1038/nn.3263.

Liu, J., Dietz, K., Hodes, G.E., Russo, S.J., Casaccia, P., 2018. Widespread transcriptional alternations in oligodendrocytes in the adult mouse brain following chronic stress. Dev. Neurobiol. 78, 152–162. https://doi.org/10.1002/dneu.22533.

Lloyd, A.F., Davies, C.L., Miron, V.E., 2017. Microglia: origins, homeostasis, and roles in myelin repair. Curr. Opin. Neurobiol. 47, 113–120. https://doi.org/10.1016/j.conb.2017.10.001.

Luo, Y., Xiao, Q., Wang, J., Jiang, L., Hu, M., Jiang, Y., Tang, J., Liang, X., Qi, Y., Dou, X., Zhang, Y., Huang, C., Chen, L., Tang, Y., 2019. Running exercise protects oligodendrocytes in the medial prefrontal cortex in chronic unpredictable stress rat model. Transl. Psychiatry 9, 322. https://doi.org/10.1038/s41398-019-0662-8.

Lupien, S.J., McEwen, B.S., Gunnar, M.R., Heim, C., 2009. Effects of stress throughout the lifespan on the brain, behaviour and cognition. Nat. Rev. Neurosci. 10, 434–445. https://doi.org/10.1038/nrn2639.

Lutz, P.E., Tanti, A., Gasecka, A., Barnett-Burns, S., Kim, J.J., Zhou, Y., Chen, G.G., Wakid, M., Shaw, M., Almeida, D., Chay, M.A., Yang, J., Larivière, V., M'Boutchou, M.N., Van Kempen, L.C., Yerko, V., Prud'Homme, J., Davoli, M.A., Vaillancourt, K., Théroux, J.F., Bramoullé, A., Zhang, T.Y., Meaney, M.J., Ernst, C., Côté, D., Mechawar, N., Turecki, G., 2017. Association of a history of child abuse with impaired myelination in the anterior cingulate cortex: convergent epigenetic, transcriptional, and morphological evidence. Am. J. Psychiatr. 174, 1185–1194. https://doi.org/10.1176/appi.ajp.2017.16111286.

Madhavarao, C.N., Moffett, J.R., Moore, R.A., Viola, R.E., Namboodiri, M.A.A., Jacobowitz, D.M., 2004. Immunohistochemical localization of aspartoacylase in the rat central nervous system. J. Comp. Neurol. 472, 318–329. https://doi.org/10.1002/cne.20080.

McEwen, B.S., Bowles, N.P., Gray, J.D., Hill, M.N., Hunter, R.G., Karatsoreos, I.N., Nasca, C., 2015. Mechanisms of stress in the brain. Nat. Neurosci. 18, 1353–1363. https://doi.org/10.1038/nn.4086.

McKenzie, I.A., Ohayon, D., Li, H., De Faria, J.P., Emery, B., Tohyama, K., Richardson, W. D., 2014. Motor skill learning requires active central myelination. Science 346, 318–322. https://doi.org/10.1126/science.1254960.

Miguel-Hidalgo, J.J., Moulana, M., Deloach, P.H., Rajkowska, G., 2018. Chronic unpredictable stress reduces immunostaining for connexins 43 and 30 and myelin basic protein in the rat prelimbic and orbitofrontal cortices. Chronic Stress 2. https://doi.org/10.1177/2470547018814186.

Milic, M., Schmitt, U., Lutz, B., Müller, M.B., 2021. Individual baseline behavioral traits predict the resilience phenotype after chronic social defeat. Neurobiol. Stress 14, 100290. https://doi.org/10.1016/j.ynstr.2020.100290.

Miller, A.H., Maletic, V., Raison, C.L., 2009. Inflammation and its discontents: the role of cytokines in the pathophysiology of major depression. Biol. Psychiatr. 65, 732–741. https://doi.org/10.1016/j.biopsych.2008.11.029.

Miyata, S., Taniguchi, M., Koyama, Y., Shimizu, S., Tanaka, T., Yasuno, F., Yamamoto, A., Iida, H., Kudo, T., Katayama, T., Tohyama, M., 2016. Association between chronic stress-induced structural abnormalities in Ranvier nodes and reduced oligodendrocyte activity in major depression. Sci. Rep. 6, 23084. https://doi.org/10.1038/srep23084.

Mosebach, J., Keilhoff, G., Gos, T., Schiltz, K., Schoeneck, L., Dobrowolny, H., Mawrin, C., Müller, S., Schroeter, M.L., Bernstein, H.G., Bogerts, B., Steiner, J., 2013. Increased nuclear Olig1-expression in the pregenual anterior cingulate white matter of patients with major depression: a regenerative attempt to compensate oligodendrocyte loss? J. Psychiatr. Res. 47, 1069–1079. https://doi.org/10.1016/j.jpsychires.2013.03.018.

Nave, K.-A., 2010. Myelination and support of axonal integrity by glia. Nature 468, 244–252. https://doi.org/10.1038/nature09614.

Nishiyama, A., Komitova, M., Suzuki, R., Zhu, X., 2009. Polydendrocytes (NG2 cells): multifunctional cells with lineage plasticity. Nat. Rev. Neurosci. 10, 9–22. https://doi.org/10.1038/nrn2495.

Pajevic, S., Basser, P.J., Fields, R.D., 2014. Role of myelin plasticity in oscillations and synchrony of neuronal activity. Neuroscience 276, 135–147. https://doi.org/10.1016/j.neuroscience.2013.11.007.

Pan, S., Mayoral, S.R., Choi, H.S., Chan, J.R., Kheirbek, M.A., 2020. Preservation of a remote fear memory requires new myelin formation. Nat. Neurosci. 23, 487–499. https://doi.org/10.1038/s41593-019-0582-1.

Poggi, G., Boretius, S., Wiebke, M., Moschny, N., Ruhwedel, T., Hassouna, I., Wieser, G. L., Werner, H.B., Goebbels, S., Nave, K.A., Ehrenreich, H., Möbius, W., Moschny, N., Baudewig, J., Ruhwedel, T., Hassouna, I., Wieser, G.L., Werner, H.B., Goebbels, S., Nave, K.A., Ehrenreich, H., 2016. Cortical network dysfunction caused by a subtle defect of myelination. Glia 64, 2025–2040. https://doi.org/10.1002/glia.23039.

Pryce, C.R., Fuchs, E., 2017. Chronic psychosocial stressors in adulthood: studies in mice, rats and tree shrews. Neurobiol. Stress 6, 94–103. https://doi.org/10.1016/j.ynstr.2016.10.001.

Rajkowska, G., Mahajan, G., Maciag, D., Sathyanesan, M., Iyo, A.H., Moulana, M., Kyle, P.B., Woolverton, W.L., Miguel-Hidalgo, J.J., Stockmeier, C.A., Newton, S.S., 2015. Oligodendrocyte morphometry and expression of myelin - related mRNA in ventral prefrontal white matter in major depressive disorder. J. Psychiatr. Res. 65, 53–62. https://doi.org/10.1016/j.jpsychires.2015.04.010.

Rohleder, N., 2014. Stimulation of systemic low-grade inflammation by psychosocial stress. Psychosom. Med. 76, 181–189. https://doi.org/10.1097/PSY.0000000000000049.

Rolls, E.T., 2019. The cingulate cortex and limbic systems for emotion, action, and memory. Brain Struct. Funct. 224, 3001–3018. https://doi.org/10.1007/s00429-019-01945-2.

Sampaio-Baptista, C., Khrapitchev, A. a, Foxley, S., Schlagheck, T., Scholz, J., Jbabdi, S., DeLuca, G.C., Miller, K.L., Taylor, A., Thomas, N., Kleim, J., Sibson, N.R., Bannerman, D., Johansen-Berg, H., 2013. Motor skill learning induces changes in

white matter microstructure and myelination. J. Neurosci. 33, 19499–19503. https://doi.org/10.1523/JNEUROSCI.3048-13.2013.
Schindelin, J., Arganda-Carreras, I., Frise, E., Kaynig, V., Longair, M., Pietzsch, T., Preibisch, S., Rueden, C., Saalfeld, S., Schmid, B., Tinevez, J.Y., White, D.J., Hartenstein, V., Eliceiri, K., Tomancak, P., Cardona, A., 2012. Fiji: an open-source platform for biological-image analysis. Nat. Methods 9, 676–682. https://doi.org/10.1038/nmeth.2019.
Sehlmeyer, C., Schöning, S., Zwitserlood, P., Pfleiderer, B., Kircher, T., Arolt, V., Konrad, C., 2009. Human fear conditioning and extinction in neuroimaging: a systematic review. PLoS One 4. https://doi.org/10.1371/journal.pone.0005865.
Seney, M.L., Huo, Z., Cahill, K., French, L., Puralewski, R., Zhang, J., Logan, R.W., Tseng, G., Lewis, D.A., Sibille, E., 2018. Opposite molecular signatures of depression in men and women. Biol. Psychiatr. 84, 18–27. https://doi.org/10.1016/j.biopsych.2018.01.017.
Sibille, E., Wang, Y., Joeyen-Waldorf, J., Gaiteri, C., Surget, A., Oh, S., Belzung, C., Tseng, G.C., Lewis, D.A., 2009. A molecular signature of depression in the amygdala. Am. J. Psychiatr. 166, 1011–1024. https://doi.org/10.1176/appi.ajp.2009.08121760.
Sierra-Mercado, D., Padilla-Coreano, N., Quirk, G.J., 2011. Dissociable roles of prelimbic and infralimbic cortices, ventral Hippocampus, and basolateral amygdala in the expression and extinction of conditioned fear. Neuropsychopharmacology 36, 529–538. https://doi.org/10.1038/npp.2010.184.
Stadelmann, C., Timmler, S., Barrantes-Freer, A., Simons, M., 2019. Myelin in the central nervous system: structure, function, and pathology. Physiol. Rev. 99, 1381–1431. https://doi.org/10.1152/physrev.00031.2018.
Steadman, P.E., Xia, F., Ahmed, M., Mocle, A.J., Penning, A.R.A., Geraghty, A.C., Steenland, H.W., Monje, M., Josselyn, S.A., Frankland, P.W., 2020. Disruption of oligodendrogenesis impairs memory consolidation in adult mice. Neuron 105, 150–164. https://doi.org/10.1016/j.neuron.2019.10.013 e6.
Süß, P., Hoffmann, A., Rothe, T., Ouyang, Z., Baum, W., Staszewski, O., Schett, G., Prinz, M., Krönke, G., Glass, C.K., Winkler, J., Schlachetzki, J.C.M., 2020. Chronic peripheral inflammation causes a region-specific myeloid response in the central nervous system. Cell Rep. 30, 4082–4095. https://doi.org/10.1016/j.celrep.2020.02.109 e6.
Tanti, A., Lutz, P.E., Kim, J., O'Leary, L., Théroux, J.F., Turecki, G., Mechawar, N., 2019. Evidence of decreased gap junction coupling between astrocytes and oligodendrocytes in the anterior cingulate cortex of depressed suicides. Neuropsychopharmacology 44, 2099–2111. https://doi.org/10.1038/s41386-019-0471-z.
Teissier, A., Le Magueresse, C., Olusakin, J., Andrade da Costa, B.L.S., De Stasi, A.M., Bacci, A., Imamura Kawasawa, Y., Vaidya, V.A., Gaspar, P., 2020. Early-life stress impairs postnatal oligodendrogenesis and adult emotional behaviour through activity-dependent mechanisms. Mol. Psychiatr. 25, 1159–1174. https://doi.org/10.1038/s41380-019-0493-2.
Treccani, G., Yigit, H., Lingner, T., Schleubner, V., Mey, F., van der Kooij, M.A., Wennström, M., Herzog, D.P., Linke, M., Fricke, M., Schmeisser, M.J., Wegener, G., Mittmann, T., Trotter, J., Müller, M.B., 2021. Early life adversity targets the transcriptional signature of hippocampal NG2+ glia and affects voltage gated sodium (Nav) channels properties. Neurobiol. Stress 15. https://doi.org/10.1016/j.ynstr.2021.100338.
Tye, K.M., Mirzabekov, J.J., Warden, M.R., Ferenczi, E.A., Tsai, H.-C., Finkelstein, J., Kim, S.-Y., Adhikari, A., Thompson, K.R., Andalman, A.S., Gunaydin, L.A., Witten, I. B., Deisseroth, K., 2013. Dopamine neurons modulate neural encoding and expression of depression-related behaviour. Nature 493, 537–541. https://doi.org/10.1038/nature11740.
Uranova, N.a., Vikhreva, O.V., Rachmanova, V.I., Orlovskaya, D.D., 2011. Ultrastructural alterations of myelinated fibers and oligodendrocytes in the prefrontal cortex in schizophrenia: a postmortem morphometric study. Schizophr. Res. Treat. 1–13. https://doi.org/10.1155/2011/325789, 2011.
Uranova, N. a, Vostrikov, V.M., Vikhreva, O.V., Zimina, I.S., Kolomeets, N.S., Orlovskaya, D.D., 2007. The role of oligodendrocyte pathology in schizophrenia. Int. J. Neuropsychopharmacol. 10, 537–545. https://doi.org/10.1017/S1461145707007626.
Uranova, N., Orlovskaya, D., Vikhreva, O., Zimina, I., Kolomeets, N., Vostrikov, V., Rachmanova, V., 2001. Electron microscopy of oligodendroglia in severe mental illness. Brain Res. Bull. 55, 597–610. https://doi.org/10.1016/S0361-9230(01)00528-7.
Urbán, N., Guillemot, F., 2014. Neurogenesis in the embryonic and adult brain: same regulators, different roles. Front. Cell. Neurosci. 8, 1–19. https://doi.org/10.3389/fncel.2014.00396.
Willner, P., 1997. Validity, reliability and utility of the chronic mild stress model of depression: a 10-year review and evaluation. Psychopharmacology (Berl) 134, 319–329. https://doi.org/10.1007/s002130050456.
Wohleb, E.S., Fenn, A.M., Pacenta, A.M., Powell, N.D., Sheridan, J.F., Godbout, J.P., 2012. Peripheral innate immune challenge exaggerated microglia activation, increased the number of inflammatory CNS macrophages, and prolonged social withdrawal in socially defeated mice. Psychoneuroendocrinology 37, 1491–1505. https://doi.org/10.1016/j.psyneuen.2012.02.003.
Wohleb, E.S., McKim, D.B., Shea, D.T., Powell, N.D., Tarr, A.J., Sheridan, J.F., Godbout, J.P., 2014. Re-establishment of anxiety in stress-sensitized mice is caused by monocyte trafficking from the spleen to the brain. Biol. Psychiatr. 75, 970–981. https://doi.org/10.1016/j.biopsych.2013.11.029.
Xiao, L., Ohayon, D., Mckenzie, I.A., Sinclair-Wilson, A., Wright, J.L., Fudge, A.D., Emery, B., Li, H., Richardson, W.D., 2016. Rapid production of new oligodendrocytes is required in the earliest stages of motor-skill learning. Nat. Neurosci. 19, 1210–1217. https://doi.org/10.1038/nn.4351.
Yang, S.M., Michel, K., Jokhi, V., Nedivi, E., Arlotta, P., 2021. Neuron class-specific responses govern adaptive myelin remodeling in the neocortex. Science 80, 370. https://doi.org/10.1126/science.abd2109.
Yang, Y., Zhang, Y., Luo, F., Li, B., 2016. Chronic stress regulates NG2+ cell maturation and myelination in the prefrontal cortex through induction of death receptor 6. Exp. Neurol. 277, 202–214. https://doi.org/10.1016/j.expneurol.2016.01.003.
Young, K.M., Psachoulia, K., Tripathi, R.B., Dunn, S.-J.J., Cossell, L., Attwell, D., Tohyama, K., Richardson, W.D., 2013. Oligodendrocyte dynamics in the healthy adult CNS: evidence for myelin remodeling. Neuron 77, 873–885. https://doi.org/10.1016/j.neuron.2013.01.006.